Are seamounts refuge areas for fauna from polymetallic nodule fields?

Daphne Cuvelier1*, Pedro A. Ribeiro1,2*, Sofia P. Ramalho1,3*, Daniel Kersken4,5, Pedro Martinez Arbizu5, Ana Colaço1

1 MARE – Marine and environmental sciences centre/IMAR – Instituto do Mar/Centro OKEANOS – Universidade dos Açores, Rua Prof. Dr. Frederico Machado 4, 9901-862 Horta, Portugal

2 Current address: Department of Biological Sciences and K.G. Jebsen Centre for Deep-Sea Research, University of Bergen, Bergen, Norway.

3 Current address: CESAM - Centro de Estudos do Ambiente e do Mar, Departmento de Biologia, Universidade de Aveiro, Campus Universitário de Santiago, 3810-193 Aveiro, Portugal

4 Department of Marine Zoology, Senckenberg Research Institute and Natural History Museum, Senckenberganlage 25, 60325 Frankfurt am Main, Germany

5 German Centre for Marine Biodiversity Research (DZMB), Senckenberg am Meer, Südstrand 44, 26382 Wilhelmshaven, Germany

* Contributed equally to this work/Corresponding authors: Daphne Cuvelier (daphne.cuvelier@gmail.com), Pedro Ribeiro (Pedro.Ribeiro@uib.no) and Sofia Pinto Ramalho (sofia.pinto.ramalho@gmail.com)

Running title: Seamounts as refuge areas for nodule fauna

Six keywords: megafauna, seamounts, nodule fields, image analysis, deep sea, mining

Abstract

Seamounts are abundant and prominent features on the deep-sea floor and intersperse with the nodule fields of the Clarion-Clipperton Fracture Zone (CCZ). There is a particular interest in characterising the fauna inhabiting seamounts in the CCZ because they are the only other ecosystem in the region to provide hard substrata besides the abundant nodules on the soft sediment abyssal plains. It has been hypothesised that seamounts could provide refuge for organisms during deep-sea mining actions or that they could play a role in the (re-)colonisation of the disturbed nodule fields. This hypothesis is tested by analysing video transects in both ecosystems, assessing megafauna composition and abundance.

Nine video transects (ROV dives) from two different license areas and one Area of Particular Environmental Interest in the eastern CCZ were analysed. Four of these transects were carried out as exploratory dives on four different seamounts in order to gain first insights in megafauna composition. The five other dives were carried out in the neighbouring nodule fields in the same areas. Variation in community composition observed among and along the video transects was high, with little morphospecies overlap on intra-ecosystem transects. Despite the observation of considerable faunal variations within each ecosystem, differences between seamounts and nodule fields prevailed, showing significantly different species associations characterising them, thus questioning their use as a possible refuge area.

1. Introduction

Seamounts are abundant and prominent features on the deep-sea floor (Wessel et al., 2010). They are common in all the world's oceans, occurring in higher abundances around mid-ocean ridges, island-arc convergent areas, and above upwelling mantle plumes (Kitchingman et al., 2007). Seamounts are defined as isolated sub-surface topographic feature, usually of volcanic origin, of significant height above the seafloor (International Seabed Authority (ISA), 2019). They are generally isolated, typically cone shaped undersea mountains rising relatively steeply at least several hundred meters from the deep-sea floor. Seamounts comprise a unique deep-sea environment, characterised by substantially enhanced currents and a fauna that is dominated by suspension feeders, such as corals (Rogers, 2018). They represent hard substrata in the otherwise soft sediment deep sea and can thus be considered habitat islands (Beaulieu, 2001). Given the growing evidence that seamounts differ substantially across a range of spatial scales, the concept of seamounts as a single, relatively well-defined habitat type is outdated (Clark et al., 2012). Depth and substrate type are key elements in determining the composition and distribution of benthic fauna on seamounts, while location is likely the subsequent most important driver of faunal composition and distribution patterns (e.g. Tittensor et al., 2009). Connectivity varies substantially between seamounts, resulting in the presence of taxa with very localised to very wide distributions (Clark et al., 2010).

The Clarion-Clipperton Fracture Zone (CCZ), in the equatorial eastern Pacific Ocean, is most known for its extensive polymetallic nodule fields that will potentially be mined in the future. In this area, nodules represent the most common hard substrate on the soft-sediment abyssal plains, and many organisms rely on them for survival (Vanreusel et al., 2016). Removal of hard substrate through mining actions will impact all these organisms, which were estimated at about 50% of all megafaunal species in the CCZ (Amon et al., 2016). Nodule fields in the CCZ are interspersed by seamounts (Wedding et al., 2013), the only feature offering hard substrata besides the nodules. Based on this feature/characteristic, it has been hypothesised that seamounts could provide refuge for organisms during deep-sea mining activities or that seamounts could play a role in the (re-)colonisation of the disturbed nodule fields. Whether or not this is true may have important implications for management of the impacts of polymetallic nodule mining in the CCZ. However, knowledge on the biodiversity inhabiting seamounts in this region is currently lacking.

The objectives of the current study were twofold: (i) Provide first insights in seamount megafauna within the CCZ, (ii) Compare the benthic fauna inhabiting seamounts and nodule fields in the eastern CCZ. Since this is the first time the seamounts at the eastern CCZ were visited, a separate section is dedicated to describe these first insights.

2. Material and Methods

2.1. Study site and data

During the SO239 ECORESPONSE cruise in 2015 (Martinez Arbizu and Haeckel, 2015), four seamounts were visited for the first time within two different license areas and one area of particular environmental interest (APEI) within the Clarion-Clipperton Fracture zone (CCZ) (Table 1). Nodule fields within the same license areas were visited and sampled as well. Video imagery and faunal samples were collected by a Remotely Operated Vehicle (ROV Kiel 6000 (GEOMAR), equipped with a high definition Kongsberg OE14-500 camera).

Seamount transects were carried out uphill, towards the summit resulting in a depth gradient along the transect (Table 1). The four seamount transects were characterised by different depth ranges and lengths and were, due to the vessel's positioning and the predominant South-East surface currents, all carried out downstream, on the north to north-western flanks of the seamounts (Table 1 and Fig. 1). The names of the seamounts used here, Rüppel and Senckenberg (BGR, German License area), Heip (GSR, Belgian License area) and Mann Borgese (APEI3), are the ones agreed upon by the scientist during the ECORESPONSE cruise (Martinez Arbizu and Haeckel, 2015), pending incorporation of these names in the GEBCO gazetteer. The seamounts differed in shape and size with Senckenberg and Heip being a sea-mountain range, while Rüppel and Mann Borgese were more isolated, stand-alone seamounts (Fig. 1). Nodule field dives were carried out on relatively flat surfaces (maximum depth range covered during a dive or transect was 30m difference, Table 1) and were referred to by the dive number and license area. The five nodule transects were all located between 4000-5000m depth and the transects differed in length between dives as well (Table 1). Within the same license area, distance between different transects was 16 to 60km, while distance between license areas added up to several hundreds of kilometres (minimum ~700kms BGR – GSR, Fig. 1).

Investigated areas were restricted to the eastern part of the CCZ with APEI3 being the most north- and westward bound area. The optical resolution of the camera enabled reliable identification of organisms larger than 3 cm (Martinez Arbizu and Haeckel, 2015). The combination of exploration and opportunistic sampling restricted a systematic image collection. Target ROV travelling altitude was <2m and travelling speed was~0.2m/s which, along with the camera zoom, were kept constant whenever possible.

2.2. Video analysis and statistics

All videos were annotated to the lowest taxonomic level possible. The number of morphospecies, defined as morphologically different organisms within the lowest taxonomic group identified, were assessed. Identifications were double checked with scientists working in the same area as well as taxonomic experts and comprise different taxonomic levels (e.g. Genus, Family) and organism samples were used for proper identification whenever possible. Those identifications restricted to higher taxon groups (Family, Class, etc.) and for which it was impossible to attribute a morphospecies, were referred to as taxa and are likely to morphologically differ between transects. Xenophyophores, living on the soft sediment deep-sea floor, were less prominently present at seamounts than at nodule fields and were not quantified. Fish (Actinopterygii), Crustacea (Nematocarcinidae, Aristeidae, Peracarida) and Polychaeta were quantified but left out of the comparing statistical analysis due to their lack of representativity and possible attraction due to ROV lights. The same was done for jellyfish and other doubtful identifications that could not be confidently assigned to a higher taxonomic group (Table A1). A subset of the nodule field transects form BGR, GSR and APEI3 was presented by Vanreusel et al. (2016), corresponding to 44% of what was studied here and limited organism identification to a higher taxonomic level (Order (e.g. Alcyonacea) or Class (e.g. Ophiuroidea)). In our study, the entire transects (100%) were annotated to morphospecies level, allowing a detailed comparison between seamounts and nodule fields.

Three categories of substratum types were distinguished: (1) Predominant soft substrata (<40% hard substrata), (2) mix or transition (between 40 and 60% hard substrata) and (3) predominant hard

substrata (>60% hard substrata), and were annotated per 10m distance units based on the video footage and tested for correlations with taxonomic abundances.

ROV transects on the seamounts were carried out as exploratory dives. Sampling strategy both at seamounts and nodule fields combined video and sampling or specimen collection. Travelling altitude was easier maintained at the relatively flat nodule field transects, where an average of 93% of the time was spent at altitudes <2m. Contrastingly, the uphill seamount transects were more variable in ROV altitude with on average 61% of the time spent at <2m altitudes, and the remaining ~39% spent at higher altitudes, which generally resulted in a higher surface covered at the seamounts. Approximate surface covered (m^2) was then estimated by using the ROV altitude, time spent at a predefined altitude, travelled distance, and the image widths at predefined altitudes. Following altitude ranges (and image widths, following Vanreusel et al. 2016 and extrapolated thereon) were taken into account: <1m (2m), 1-2 m (4m), 2-3m (6m), 3-4 m (8m), 4-5m (10m). Ranges from >5m, adding up to 12% for seamount transects and 3% for nodule field transects that were left out since these were the parts were the seafloor was not visualised or organisms could not be quantified. Due to the explorative nature of the dives, the pan and tilt of the ROV camera were not kept constant and thus represents a bias on the surface estimations. Visualisation of ancient disturbance tracks were omitted as well, as these fell out of the scope of the article. Faunal densities were calculated as individuals per square meter (ind./$100m^2$). Statistical testing was carried out in R (R core team, 2018). Non-metric multidimensional scaling analysis (NMDS) was based on Bray-Curtis dissimilarity and carried out with the vegan package (Oksanen et al., 2018). The Kendall's coefficient of concordance (W) was calculated to identify significantly associated groups of species, based on correlations and permutations (Legendre, 2005).

3. Results

About 80% of all taxa observed across the two adjacent ecosystems, could be identified to a morphospecies level. At a first view, morphospecies revealed to be quite different between seamounts and nodule fields (Fig. 2). While the number of faunal observations at the seamount transects were within similar ranges (4.4-7.6 ind./$100m^2$), those at the nodule transects featured both highest and lowest values (3.8-30.3 ind./$100m^2$) (Table 1). The lowest number of faunal observations were done at the two APEI3 nodule transects (ROV13 and 14) and highest at the GSR nodule transect ROV08. What follows is a first description of eastern CCZ seamount megafauna (section 3.1.) and a detailed comparison with the neighbouring nodule fields (section 3.2.)

3.1. Insights in CCZ seamount megafauna

The most abundant and diverse (most morphospecies) taxa at the seamount transects comprised Echinodermata (Asteroidea, Crinoidea, Holothuroidea and Ophiuroidea), Anthozoa (Actiniaria, Alcyonacea, Pennatulacea) and Porifera (Hexactinellida) (Table A1, Fig. 3, Fig. A1). Keeping in mind the limitation of the video sampling, differences among the benthic seamount community composition are described here. The transect at Mann Borgese (APEI3) was characterised by high densities of Antipatharia, more specifically Antipathidae (3.5 ind./$100m^2$), and solitary Scleractinia (1.5 ind./$100m^2$) (Table A1, Fig. 3). Antipathidae observations were mostly grouped at the end of the video transect, i.e. at the summit. Densities of both Antipatharia and Scleractinia were much lower on the other seamount transects (<0.2 ind./$100m^2$) with Scleractinia being absent from Heip and Senckenberg transects. Alcyonacea corals were observed on all seamount transects. Isididae were found at Senckenberg and Heip transects, and one individual from the Chrysogorgiidae family was observed at the latter as well. Varying numbers of Primnoidae were observed on all transects (Table

A1). High abundances of Pennatulacea were observed at Senckenberg (0.7 ind./100m^2), representing about 20% of sessile fauna annotations for this transect.

Enteropneusta were only observed on Rüppel and Senckenberg transects in the BGR area, represented by two different morphospecies, namely *Yoda* morphospecies (Torquaratoridae) at Rüppel and *Saxipendium* morphospecies (Harrimaniidae) at Senckenberg.

Highest Polychaeta densities were observed at Heip transect in the GSR area, which was mainly due to high densities of free-swimming Acrocirridae (0.5 ind./100m^2 vs. 0.02-0.03ind./100m^2 in BGR area Table A1). Aphroditidae polychaetes were only present at the BGR transects (0.02 ind./100m^2 , corresponding to 3 individuals along the transect at Rüppel and 1 individual along the transect at Senckenberg) (Table A1).

Porifera densities were highest at the Heip transect (0.93 ind./100m^2), followed by Senckenberg (0.38 ind./100m^2), Mann Borgese (0.36 ind./100m^2) and lastly Rüppel (0.31 ind./100m^2) (Table 2, Fig. A1(c)). Six Porifera families were annotated featuring >7 to >10 morphospecies per transect (Table 2). Cladorhizidae (two individuals) were only observed on Heip transect, and one *Poliopogon* sp. (Pheronematidae) was observed at Mann Borgese transect. Rossellidae gen. sp. nov. was present on three seamount transects, exception being Mann Borgese.

Overall Echinodermata densities were highest at Senckenberg seamount (3.5 ind./100m^2), adding up to 51% of all image annotations for this transect. For comparison, echinoderms at Heip (1.5 ind./100m^2) and Rüppel (1.4 ind./100m^2) were responsible for 37 and 32% of all image annotations for these transects, followed by Mann Borgese (0.62 ind./100m^2) or 8.2% of the annotations. The number of morphospecies for all echinoderm taxa (Asteroidea, Echinoidea, Holothuroidea and Crinoidea) was also highest at these 2 seamounts in the BGR area (Fig. A1., Table A1). Crinoidea and Holothuroidea densities were highest at Senckenberg (0.9 ind./100m^2 and 0.7 ind./100m^2, respectively). The holothuroid families of Elpidiidae and Laetmogonidae were only observed at Senckenberg and Rüppel (BGR). Psychropotidae and Synallactidae were observed on all seamounts, represented by different morphospecies. Deimatidae were not observed on Mann Borgese, but were present on the three other seamount transects, again with different morphospecies and densities. Velatid Asteroidea were only observed at Senckenberg and Rüppel (BGR), while Brisingida and Paxillosida were observed on all four seamounts. Aspidodiadematid Echinoidea were absent from the Heip transect and urechinid Echinoidea were absent from the Mann Borgese transect.

A species accumulation curve (Fig. 4a) confirmed the limitations of the restricted and exploratory nature of the sampling as no asymptote was reached. The rarefaction curves (Fig. 4b) showed that the transects with the most faunal observations, which corresponded here to the longer transects, were more diverse. However, at smaller sample sizes curves did not cross, thus maintaining the differences observed at higher sample sizes with the Senckenberg transect (ROV04) as most diverse followed by Rüppel (ROV02) (both BGR). The video transect carried out at Mann Borgese (ROV15, APEI3) was the least diverse.

A comparison of all morphospecies observed along the 4 transects was presented in a Venn diagram (Fig. 5a). Each seamount transect was characterised by a highest number of unique morphospecies,

only observed on the transect in question and not elsewhere. Only three morphospecies were present in all seamount transects, namely Ceriantharia msp. 2, a small red galatheid crab and a foliose sponge. Highest number of overlapping morphospecies (n=16) was observed between Rüppel and Senckenberg, both in the BGR area (Fig. 5a). Mann Borgese showed the smallest degree of overlap with the other transects (Fig. 5a).

About 57% of all sessile fauna was associated with predominantly hard substrata, followed by 31% on the mixed substrata. For the mobile taxa, the pattern was less pronounced with 41 and 42% associated with predominantly hard and mixed hard/soft substrata respectively. The amount of predominantly hard and soft substrata was negatively correlated, though not significantly. This was due to the equal amounts (40-60%) of mixed hard/soft substrata. Over all seamount transects pooled together, no taxa were significantly correlated with the amount of hard substrata, nor with soft substrata. When looking at the individual transects, no significant correlations were found between taxa and substrata for ROV02 or ROV04 or ROV09, most likely due to the equal distribution of the amount of hard/soft/mix substrata. In this perspective, ROV15 stood out, as it was dominated by predominantly hard substrata (56/%). For this transect, Pennatulacea were significantly negatively correlated with the amount of hard substrata and Zoantharia/Octocorralia were significantly and positively correlated with hard substrata, as were Ophiuroidea, Asteroidea, Crinoidea and Mollusca.

Due to the limited sample size, the representativity of the observed biological patterns remains to be corroborated by a more elaborate sampling strategy.

3.2. Comparison of seamount and nodule field faunal composition and variation

The faunal composition and richness of the nodule transects can be consulted in Fig. 3, Fig. A1 and Table A1. The only taxon showing significant difference in density between seamounts and nodule fields were the Porifera (T-test assuming unequal variances, $t=-3.7$, $p<0.05$). In concordance with the seamount transect, the species accumulation curve of the nodule transects did not reach an asymptote either (Fig. 4c). The rarefaction curves showed that the relations among transects were less straightforward for the nodule transects versus the seamount ones and did cross at smaller sample sizes (<100 individuals, Fig. 4d). ROV13 and ROV14 transects (both APEI3) were the longest in distance travelled (Table 1) but featured less faunal observations. At small sample sizes, the richness at ROV13 and 14 was highest. ROV08 and ROV10 (both GSR) showed parallel curves with ROV08 being more diverse (Fig. 4d).

A venn diagram showing the morphospecies overlap among the nodule transects showed a total of 5 species re-occurring on all 5 transects (Fig. 5b). These were: Munnopsidae msp. 1 (Isopoda, Crustacea), Actiniaria msp.7 (Cnidaria), Ophiuroidea msp. 6 (Echinodermata), *Holascus* sp. and *Hyalonema* sp. (Hexactinellida, Porifera). There was a high number of unique morphospecies for each transect, though not as high as for the seamount transects (Fig. 5). ROV13 and 14 (both APEI3) showed least overlap with the other transects, which is similar to what was observed at the seamounts.

Observations and quantifications of morphospecies confirmed the high degree of dissimilarity between the two neighbouring ecosystems. Porifera, Ophiuroidea (Echinodermata), Actiniaria and Alcyonacea (Cnidaria) were more abundant at nodule fields (Fig. 3). These taxonomic groups were also most diverse on nodule fields (i.e. highest number of morphospecies), exception being the Alcyonacea which featured more morphospecies on the seamounts (12 to 8 morphospecies for

seamounts and nodule fields respectively) (Fig. 3). Of all Porifera, Cladhorizidae were more diverse at nodule fields than at seamounts (7 to 1 morphospecies, respectively).

There were only 21 morphospecies (10%) that were observed both on seamounts and nodule fields (Fig. 6). While this subset of morphospecies occurred in both ecosystems, they did so in very different densities, i.e. very abundant in one ecosystem and very low in abundance in the other: examples are Galatheidae small red msp. (Decapoda, Crustacea), *Synallactes* white msp. (Holothuroidea), Ophiuroidea msp. 5 and 6, Comatulida msp. 1 (Crinoidea), *Hyalonema* sp. and *Hyalostylus* sp. (both Hexactinellida, Porifera) (Fig. 6).

Three Ophiuroidea morphospecies were present at both seamounts and nodule fields (Fig. 2, 3 and 6). Most of the Ophiuroidea observed at the CCZ seamounts that could be identified to morphospecies level, were small and situated on hard substrata (morphospecies 5), while those at nodule fields (including morphospecies 6) were observed on the soft sediments. Morphospecies 6 was only rarely observed on the seamounts (Fig. 3). Another easily recognisable morphospecies was found on Porifera, coral and animal stalks and was more abundant at seamounts than at nodule fields (morphospecies 4) (Fig. 3).

Crinoidea, Asteroidea (both Echinodermata) and Antipatharia (Cnidaria) were more abundant on the seamounts (Fig. 3). This coincided with a higher diversity for Asteroidea and Antipatharia on the seamounts as well. Crinoidea diversity was similar (5 to 4 morphospecies comparing seamounts to nodule fields). Holothuroidea occurred in similar densities in both ecosystems (Fig. 3, though they were characterised by different morphospecies (Table 2, Fig. A1(b)). Overall densities of Echinoidea were comparable between seamounts and nodule fields, though for the nodule fields this was mostly due to one very abundant morphospecies, namely Aspidodiadematidae msp 1, which was absent at the seamounts (Table 2, Fig. A1(b)). Besides this, Echinoidea were more diverse at seamounts (11 morphospecies vs. 5 at nodule fields).

There was no morphospecies overlap for Tunicata, Antipatharia, and Actiniaria. Alcyonacea, Ceriantharia, Corallimorphidae and Crinoidea only shared 1 morphospecies between seamounts and nodule fields, namely *Callozostron* cf. *bayeri*, Ceriantharia msp. 2, *Corallimorphus* msp. 2 and Comatulida msp. 1 respectively (Fig. 6).

There were no observations of Enteropneusta, Scleractinia and Zoantharia (Cnidaria), Aphroditidae (Polychaeta) or holothuroid Deimatidae at the nodule fields transects (Table A1, Fig. A1). While Actinopterygii were left out of the analysis, it should be noted that fish observations were more diverse at the seamounts than on the nodule fields.

There was quite some faunal variation observed among the video transects of, both seamounts and nodule fields (see Fig. 5 and 7). The (dis)similarities were analysed by a nMDS analysis, which grouped the 9 different video transects based on their taxonomic composition. Despite the large intra-ecosystem variation, they pooled in two distinct groups separating the nodule fields from the seamounts (Fig. 7a). Within each group, BSR and GSR transects were more similar to one another both for seamounts and nodule fields, whilst APEI3 transects stood out more.

The Kendall's coefficient of concordance (W, Legendre, 2005) corroborated the existence of two significantly different species associations, whose composition corresponded to the fauna

characterising the nodule fields (W=2.03, p<0.001, after 999 permutations) and the seamounts (W=3.04, p<0.001, after 999 permutations).

Depth was fitted as a vector on top of the nMDS plot (Fig. 7b) and showed that the discrepancy in faunal composition between the two ecosystems also corresponded to a difference in depth, with the nodule transects all being situated below the 4000m isobath and the seamount transects ranging from 1650 to >3500m (Fig. 7b).

4. Discussion

4.1. Intra-ecosystem faunal variation

Community composition varied markedly at seamounts and nodule fields. The limited sampling (n=9 transects), at different locations and additionally, for the seamounts, different depth ranges, precluded any general conclusions on quantifications of biodiversity *per se*. However, taking this into account, it was also the first time seamounts were visited in the area, thus granting first insights in the fauna inhabiting these seamounts and allowing a first comparison with nodule faunal composition.

The two BGR seamount transects were most similar in faunal composition, followed by the Heip seamount transect (GSR). These seamount video transects were characterised by more similar depth ranges, and the two BGR transects were also geographically closest to each other. Although for seamounts, distance separating them might be a less determining factor than depth since (mega)faunal communities can be very different even between adjacent seamounts (Schlacher et al., 2014; Boschen et al., 2015). Overall, parameters that vary with depth, such as temperature, oxygen concentration, substratum type, food availability, and pressure are considered major drivers of species composition on seamounts (Clark et al., 2010; McClain et al., 2010). The quantification of the amount of hard and soft substrata was not distinctive enough to explain differences observed here. The difference in depth could also explain the higher dissimilarity with Mann Borgese (APEI3) who featured the shallowest transect and summit, which was dominated by Antipatharia. Antipatharians were previously reported to be more dominant towards peaks as compared to mid-slopes at corresponding depths (Genin et al., 1986). Based on their filter-feeding strategy, Porifera (except carnivorous Cladorhizidae), were also thought to benefit from elevated topography (peaks) or exposed substrata in analogy to corals (Genin et al., 1986; Clark et al., 2010), though no such pattern was apparent here. Porifera are notoriously difficult to identify based on imagery. Although the sampled individuals allowed some identifications to genus or species level (Kersken et al., 2018a and b), identifications remained hard to extrapolate across the different video transects. Generally, as in our study, seamount summits have been more intensively sampled (Stocks, 2009) although the little work done at seamount bases and deep slopes indicated that these areas support distinct assemblages (Baco, 2007).

Among the nodule transects a considerable amount of variation in faunal composition was observed (this study, Vanreusel et al., 2016). The two APEI3 nodule transects (ROV13 and 14) stood out in faunal composition, diversity and in low number of faunal observations. They were also the only two transects situated below the 4500m isobaths. But rather than depth, the nodule coverage may be considered an important driving factor, since the density of nodule megafauna was shown to vary with nodule size and density/coverage (Stoyanova, 2012; Vanreusel et al., 2016, Simon-Llédo et al., 2019). Here as well, the APEI3 transects were characterised by a high nodule coverage (~40-88%,

Vanreusel et al., 2016), whereas the BGR and GSR nodule transects (ROV3 and ROV 8 + 10, respectively) had a nodule coverage <30% and were also more similar in faunal composition (Vanreusel et al., 2016). Other factors that could be at play are the more oligotrophic surface waters of the northern CCZ which could be the cause of the overall lower faunal densities at APEI3 nodule fields (Vanreusel et al., 2016). Volz et al. (2018) corroborated this, with the location of the APEI3 site in the proximity of the carbon-starved North Pacific gyre being characterised by a reduced POC-flux quantified to being 22-46% lower than the GSR and BGR areas respectively.

The species accumulation curves showed that an asymptote was reached neither at seamounts, nor at nodule fields. Consequently, longer transect lengths might be necessary to representatively quantify and assess megafauna density and diversity (Simon-Lledó et al., 2019). In addition, for a first in-depth description and assessment of seamount fauna composition, one video transect is insufficient to describe the diversity and shifts in faunal assemblages of the surveyed seamounts. Rather, an ampler imaging strategy should be developed, with a minimum transect length exceeding 1000 m (Simon-Llédo et al., 2019) and replicate transects carried out on different faces of the seamount, on slopes with varying degree of exposure to currents and different substrate types. Wider depth ranges should be taken into account as well. Alternatively, across slope transects, following depth contours should be considered as these could provide observation replicates for a given depth. Despite its limitations, this study grants first insights in the seamount inhabiting megafauna of the eastern CCZ and an important first comparison with nodule fauna.

4.2. Faunal (dis)similarities between seamounts and nodule fields

In other areas, seamounts were shown to share fauna with surrounding habitats (Clark et al., 2010) and could thus potentially serve as source populations for neighbouring environments (McClain et al., 2009). While generally few species seemed restricted to seamounts only (Clark et al., 2010), morphospecies in this study revealed to be quite different between seamounts and nodule fields with little overlap between both. Despite the high degree of variation observed among all the video transects, these grouped into two distinctly separate clusters, separating nodule from seamount transects. The few overlapping morphospecies did occur in different densities in each ecosystem, implying a different role or importance in the ecological community and its functioning.

Overall, nodule fields showed higher faunal densities than seamounts. Shifts in density patterns between nodule fields and seamounts were more evident in a number of taxa, where the variety of morphospecies and feeding strategy within each group was likely to be at play. An example of this are the Echinodermata, which include Asteroidea (predators and filter feeders (Brisingida)), Crinoidea (filter feeders), Echinoidea (deposit feeders), Holothuroidea (deposit feeders) and Ophiuroidea (omnivores). Asteroidea were more abundant on seamounts and both Echinoidea and Asteroidea were more diverse in this ecosystem as well. Ophiuroidea were most abundant on the nodule fields (ratio 7 to 1 when compared to seamounts). Same ophiuroid morphospecies were present at seamounts and nodule fields but in very different abundances and they were observed on different substrata types, which indicates different lifestyles, feeding behaviour and corresponding dietary specialisations (Persons and Gage, 1984). Previously it was already demonstrated that Ophiuroidea did not show high levels of richness or endemism on seamounts (O'Hara, 2007). At nodule fields, Ophiuroidea were often observed in association with xenophyophores (Amon et al., 2016, this study) and a similar observation was done at east Pacific seamounts off Mexico (Levin et al., 1986), though no such associations were observed on the seamounts studied here.

Holothuroidea densities were thought to possibly decrease when less soft sediment was available since they feed mainly on the upper layers of the soft-bottom sediment (Bluhm and Gebruk, 1999). No significant link was established between holothuroid densities and the amount of hard substrata in this study, but their community composition varied distinctly between nodule fields and seamounts with more families being observed at the latter. Additionally, at the seamounts, many holothurians were observed on top of rocks, possibly reflecting different feeding strategies and explaining the observations of different morphospecies. Geographical variations, different bottom topography, differences in nodule coverages and sizes and/or an uneven distribution of holothurians on the sea floor were thought to play a role in holothuroid community composition (Bluhm and Gebruk, 1999). On the other hand, variability in deep-sea holothuroid abundance was proposed to depend primarily on depth and distance from continents (see Billet, 1991 for a review).

Stalked organisms, such as Crinoidea (Echinodermata) and Hexactinellida (except for Amphidiscophora, Porifera) rely on hard substrata for their attachment and are considered being among the most vulnerable organisms when mining is concerned. Crinoidea were more abundant on seamounts, possibly because hard substrata were less limiting than in the nodule fields. Porifera densities (stalked and non-stalked) varied among all analysed transects, revealing no particular trends in abundance. However, the species composition of deep-sea glass sponge communities from seamounts and polymetallic nodule fields was distinctly different. Polymetallic nodule field communities were dominated by widely-distributed genera such as *Caulophacus* and *Hyalonema*, whereas seamount communities seemed to have a rather unique composition represented by genera like *Saccocalyx*.

Corals were generally considered to be more abundant on seamounts than adjacent areas, due to their ability to feed on a variety of planktonic or detritus sources suspended in the water column (Rowden et al., 2010). In this study, the Alcyonacea densities were lower on the seamounts than on the nodule transects. The majority of Alcyonacea morphospecies of the seamounts did not occur on the nodule fields and vice versa, with exception of *Callozostron* cf. *bayeri* which was also present at the nodule fields but in very low densities (1/8 of those observed at seamounts). The Antipatharia were most abundant at the Mann Borgese seamount (APEI3) compared to all other transects. The depth difference of more than 3000m between this particular seamount and the nodule fields could explain the abundance in Antipatharia which were shown to be more abundant at lower depths (Genin et al., 1986). Additional presence of Pennatulacea at seamounts, a taxon that was virtually absent from the nodule field transects and that appeared more linked to predominant soft substrata at seamounts, resulted in completely distinct coral communities for each ecosystem.

Actiniaria were denominated the second most common group at CCZ nodule fields, after the xenophyophores (Kamenskaya et al., 2015) and, in our study, were also more abundant on nodule fields than on seamounts. Depending on the species and feeding strategy, the ratio hard/soft substrata and their preference for either one could play a role. Since morphospecies were distinct between seamounts and nodule fields, their role in the respective communities are likely to differ as well. Combinations of deposit feeding and predatory behaviour in Actiniaria have been observed, as well as burrowing activity, preference for attachment to hard substrata and exposure to currents (Durden et al., 2015a; Lampitt and Paterson, 1987; Riemann-Zürneck, 1998), all factors that could influence the differences in morphospecies observed.

Some taxa were only observed on the seamounts in this study, while they occurred on nodule fields elsewhere, be it in low densities. For instance, Enteropneusta, which in this study were found only on seamounts, were observed previously at CCZ nodule fields though observations were rather rare (Tilot, 2006). They appeared more abundant at the nodule fields of the Deep Peru Basin (DISCOL area), though a wide range in abundances was displayed there as well (Bluhm, 2001). The exception were the Scleractinia, which were quite common on seamounts, as also reported in other studies (e.g. Baco, 2007, Rowden et al., 2010), but distinctly absent at nodule fields.

Explanation for the discrepancies in faunal composition and the low degree of morphospecies overlap between seamount and nodule fields, as observed here, can be multiple. For one, nodules may not be considered a plain hard substratum, with their metal composition, microbial colonisation and the nodule/sediment interface influencing the epi-and associated megafaunal composition. The possibility of a specific deep-sea faunal community that tolerates or benefits from manganese substrata has been previously proposed (Mullineaux, 1988). The comparison between seamounts and nodule fields as two neighbouring hard-substrata ecosystems also entailed a comparison between depth gradients and possible thresholds (>4000m for nodule fields and 1500>x <4000m for seamounts). Related to this is the steepness of the seamount slope and its current exposure playing a role in the faunal colonisation (Genin et al., 1986; Rappaport et al., 1997). Other studies showed that habitat heterogeneity increased megafaunal diversity at seamounts (Raymore, 1982) and elsewhere, such as abyssal plains (Lapointe and Bourget, 1999; Durden et al., 2015b, Leitner et al., 2017, Simon-Llédo et al., 2019). Within this perspective the smaller-scale substratum heterogeneity transcending the ratio hard/soft substrata or amount of hard substrata could play a role as well.

5. Conclusions

Based on our current knowledge; seamounts appear inadequate as refuge areas to help maintain nodule biodiversity. In order to conclusively exclude seamount habitats as a refuge for nodule fauna, a more comprehensive sampling should be carried out. The sampling strategy wielded in this study lacked replicates, uniformity and was limited in sample size. Seamount bases should be taken into consideration as well as they can be characterised by distinctly different assemblages than the summits and they feature depth ranges more similar to nodule fields.

While their role as refuge area for nodule field fauna is currently debatable, the possible uniqueness of the seamount habitat and its inhabiting fauna implies that seamounts need to be included in management plans for the conservation of the biodiversity and ecosystems of the CCZ.

Author Contributions

DC, PAR, SPR, DK analysed the images. DC analysed the data. PMA, PAR, AC conceptualised and carried out the sampling. All authors contributed to the redaction of the manuscript.

Data Availability

Data sets are made available through OSIS-Kiel data portal, BIIGLE and PANGAEA.

Competing interest

The authors declare that they have no conflict of interest

Acknowledgments

We thank the crew of SO239 and GEOMAR for their support in acquiring the images used in this article. The EcoResponse cruise with RV Sonne was financed by the German Ministry of Education and Science BMBF as a contribution to the European project JPI-Oceans "Ecological Aspects of Deep-Sea Mining". This study had the support of PO AÇORES 2020 project Acores-01-0145-Feder-000054_RECO and of Fundação para a Ciência e Tecnologia (FCT), through the strategic projects UID/MAR/04292/2013 granted to MARE. The authors acknowledge funding from the JPI Oceans—Ecological Aspects of Deep Sea Mining project by Fundação para a Ciência e Tecnologia de Portugal (Mining2/0005/2017) and the European Union Seventh Framework Programme (FP7/2007–2013) under the MIDAS project, grant agreement n° 603418. DC is supported by a post-doctoral scholarship (SFRH/BPD/110278/2015) from FCT. PAR was funded by the Portuguese Foundation for Science and Technology (FCT), through a postdoctoral grant (ref. SFRH/BPD/69232/2010) funded through QREN and COMPETE. SPR is supported by FCT in the scope of the "CEEC Individual 2017" contract (CEECIND/00758/2017) and by CESAM (UIDP/50017/2020+UIDB/50017/2020), through national funds from FCT/MCTES. AC is supported by Program Investigador (IF/00029/2014/CP1230/CT0002) from FCT. PMA acknowledges funding from BMBF contract 03 F0707E. Pictures were provided by GEOMAR (Kiel).

References

Amon, D. J., Ziegler, A. F., Dahlgren, T. G., Glover, A. G., Goineau, A., Gooday, A. J., Wiklund, H., and Smith, C. R.: Insights into the abundance and diversity of abyssal megafauna in a polymetallic-nodule region in the eastern Clarion-Clipperton Zone. Sci. Rep., 6(1), 30492. https://doi.org/10.1038/srep30492, 2016

Baco, A.R. : Exploration for deep-sea corals on North Pacific seamounts and islands. Oceanography 20:109– 17, 2007

Beaulieu, S. E.: Colonization of habitat islands in the deep sea: Recruitment to glass sponge stalks. Deep-Sea Res Pt I, 48(4), 1121–1137. https://doi.org/10.1016/S0967-0637(00)00055-8, 2001

Bluhm, H.: Re-establishment of an abyssal megabenthic community after experimental physical disturbance of the seafloor. Deep-Sea Res Pt II, 48(17–18), 3841–3868. https://doi.org/10.1016/S0967-0645(01)00070-4, 2001

Bluhm, H., and Gebruk, A. V.: Holothuroidea (Echinodermata) of the Peru basin - ecological and taxonomic remarks based on underwater images. Mar. Ecol., 20(2), 167–195. https://doi.org/10.1046/j.1439-0485.1999.00072.x, 1999

Boschen, R. E., Rowden, A. A., Clark, M. R., Barton, S., Pallentin, A., and Gardner, J.:Megabenthic assemblage structure on three New Zealand seamounts: implications for seafloor massive sulfide mining. Mar. Ecol. Prog. Ser., 523, 1–14. https://doi.org/10.3354/meps11239, 2015

Clark, M. R., Rowden, A. A., Schlacher, T., Williams, A., Consalvey, M., Stocks, K. I., Rogers,A.D., O'Hara, T.D., White, M., Shank, T.M., and Hall-Spencer, J. M.: The Ecology of Seamounts: Structure, Function, and Human Impacts. Annu. Rev. Mar. Sci., 2(1), 253–278. https://doi.org/10.1146/annurev-marine-120308-081109, 2010

Clark, M.R., Schlacher, T.A., Rowden, A.A., K. Stocks, K.I., and Consalvey, M.: Science priorities for seamounts: research links to conservation and management. PLoS One 7(1): e29232., 2012

Durden, J. M., Bett, B. J., and Ruhl, H. A.: The hemisessile lifestyle and feeding strategies of *Iosactis vagabunda* (Actiniaria, Iosactiidae), a dominant megafaunal species of the Porcupine Abyssal Plain. Deep-Sea Res Pt I 102, 72–77. https://doi.org/10.1016/j.dsr.2015.04.010, 2015a

Durden, J. M., Bett, B. J., Jones, D. O. B., Huvenne, V. A. I., and Ruhl, H. A.: Abyssal hills - hidden source of increased habitat heterogeneity, benthic megafaunal biomass and diversity in the deep sea. Prog. Oceanogr., 137, 209–218, https://doi.org/10.1016/j.pocean.2015.06.006, 2015b

Genin, A., Dayton, P. K., Lonsdale, P., and Spiess, F. N.: Corals on seamount peaks provide evidence

of current acceleration over deep-sea topography. *Nature*, *322*, 59–61, 1986
International Seabed Authority (ISA): https://www.isa.org.jm/scientific-glossary/, last access: 29 October 2019
Kamenskaya, O. E., Gooday, A. J., Tendal, O. S., and Melnik, V. F.: Xenophyophores (Protista, Foraminifera) from the Clarion-Clipperton Fracture Zone with description of three new species. Mar. Biodivers., 45(3), 581–593. https://doi.org/10.1007/s12526-015-0330-z, 2015
Kersken, D., Janussen, D., and Martinez Arbizu, P.: Deep-sea glass sponges (Hexactinellida) from polymetallic nodule fields in the Clarion-Clipperton Fracture Zone (CCFZ), northeastern Pacific: Part I – Amphidiscophora. Mar. Biodivers. 48, 545–573.https://doi.org/10.1007/s10750-017-3498-3, 2018a
Kersken, D., Janussen, D., and Martinez Arbizu, P.: Deep-sea glass sponges (Hexactinellida) from polymetallic nodule fields in the Clarion-Clipperton Fracture Zone (CCFZ), northeastern Pacific: Part II—Hexasterophora. Mar. Biodivers. https://doi.org/https://doi.org/10.1007/s12526-018-0880-y, 2018b
Lampitt, R. S., and Paterson, G. L. J.: The feeding behaviour of an abyssal sea anemone from in situ time lapse photographs and trawl samples. Oceanol. Acta, 10(4), 455–461, 1987
Lapointe, L., and Bourget, E.: Influence of substratum heterogeneity scales and complexity on a temperate epibenthic marine community. Mar. Ecol. Prog. Ser., 189(2), 159–170. https://doi.org/10.3354/meps189159, 1999
Leitner, A. B., Neuheimer, A. B., Donlon, E., Smith, C. R., and Drazen, J. C.: Environmental and bathymetric influences on abyssal bait-attending communities of the Clarion Clipperton Zone. Deep-Sea Res Pt I, 125, 65–80. https://doi.org/10.1016/j.dsr.2017.04.017, 2017
Levin, L., DeMaster, D., McCann, L., and Thomas, C.: Effects of giant protozoans (class: Xenophyophorea) on deep-seamount benthos. Mar. Ecol. Prog. Ser., 29, 99–104. https://doi.org/10.3354/meps029099, 1986
McClain, C. R., Lundsten, L., Barry, J., and DeVogelaere, A.: Assemblage structure, but not diversity or density, change with depth on a northeast Pacific seamount. Mar. Ecol., 31, 14–25. https://doi.org/10.1111/j.1439-0485.2010.00367.x, 2010
McClain, C. R., Lundsten, L., Ream, M., Barry, J., and DeVogelaere, A.: Endemicity, biogeography, composition, and community structure on a Northeast Pacific seamount. PLoS ONE, 4(1). https://doi.org/10.1371/journal.pone.0004141, 2009
Mullineaux, L.S.: The role of settlement in structuring a hard-substratum community in the deep sea. J. Exp. Mar. Biol. Ecol. 120, 241-261, 1988
O'Hara, T. D.: Seamounts: Centres of endemism or species richness for ophiuroids? Glob. Ecol. Biogeogr., 16(6), 720–732. https://doi.org/10.1111/j.1466-8238.2007.00329.x, 2007
Oksanen, J., Blanchet, G., Friendly, M., Kindt, R., Legendre, P., McGlinn, D., Minchin, P.R., O'Hara, R.B., Simpson, G.L., Solymos. P., Stevens, M.H.H., Szoecs, E., and Wagner, H.: vegan: Community Ecology Package. R package version 2.5-2. https://CRAN.R-project.org/package=vegan, 2018
Rappaport, Y., Naar, D. F., Barton, C. C., Liu, Z. J., and Hey, R. N.: Morphology and distribution of seamounts surrounding Easter Island. J. Geophys. Res., 102(B11), 24713. https://doi.org/10.1029/97JB01634, 1997
R Core Team: R: A language and environment for statistical computing. R Foundation for Statistical Computing, Vienna, Austria. URL https://www.R-project.org/, 2018
Riemann-Zürneck, K.: How sessile are sea anemones? A review of free-living forms in the Actiniaria (Cnidaria: Anthozoa). Mar. Ecol., 19(4), 247–261. https://doi.org/10.1111/j.1439-0485.1998.tb00466.x, 1998
Rogers, A.D.: The Biology of Seamounts: 25 years on. Adv. Mar. Biol. 79, 137-224, https://doi.org/10.1016/bs.amb.2018.06.001, 2018
Rowden, A.A., Schlacher, T.A., Williams, A., Clark, M.R., Stewart, R., Althaus, F., Bowden, D.A., Consalvey, M., Robinson, W. and Dowdney, J.: A test of the seamount oasis hypothesis: seamounts support higher epibenthic megafaunal biomass than adjacent slopes. Mar Ecol, 31,

95-106, https://doi.org/10.1111/j.1439-0485.2010.00369.x, 2010
Simon-lledó, E., Bett, B. J., Huvenne, V. A. I., Schoening, T., Benoist, N. M. A., Je, R. M., Durden, J.M, and Jones, D. O. B.: Megafaunal variation in the abyssal landscape of the Clarion Clipperton Zone, Progr. Oceanogr. 170, 119–133. https://doi.org/10.1016/j.pocean.2018.11.003, 2019
Tilot, V., Ormond, R., Moreno Navas, J., and Catalá, T. S.: The Benthic Megafaunal Assemblages of the CCZ (Eastern Pacific) and an Approach to their Management in the Face of Threatened Anthropogenic Impacts. Front Mar Sci., 5, 1–25. https://doi.org/10.3389/fmars.2018.00007, 2018
Vanreusel, A., Hilario, A., Ribeiro, P. A., Menot, L., and Arbizu, P. M.: Threatened by mining, polymetallic nodules are required to preserve abyssal epifauna. Sci. Rep., 6(1), 26808. https://doi.org/10.1038/srep26808, 2016
Wedding, L. M., Friedlander, A. M., Kittinger, J. N., Watling, L., Gaines, S. D., Bennett, M., Hardy, S.M., and Smith, C.R.: From principles to practice : a spatial approach to systematic conservation planning in the deep sea. Proc. R. Soc. B 280: 20131684. http://dx.doi.org/10.1098/rspb.2013.1684, 2013
Wessel, P., Sandwell, D., and Kim, S.-S.: The Global Seamount Census. Oceanography 23(1), 24–33, https://doi.org/10.5670/oceanog.2010.60, 2010

Tables

Table 1. Overview table on details of imagery transects analysed in the Clarion-Clipperton license areas. Video duration includes time spent sampling. Number of observations include undetermined organisms. Transect lengths do not include parts visualising ancient disturbance tracks or parts when the seafloor was not visualised or visible.

Station/Dive	License Area	Seamount (SM) or Nodule field (NF)	Depth (m)	Transect length	Approximate surface covered (m^2)	Faunal densities (ind. /100m^2)
SO239_29_ROV02	BGR	SM: Rüppell	3000-2500	1250m	9458.6	4.4
S0239_41_ROV03	BGR	NF	4080-4110	1590m	5309.1	19.3
SO239_54_ROV04	BGR	SM: Senckenberg	3350-2850	2500m	12288.5	6.9
S0239_131_ROV08	GSR	NF	4470-4480	710m	1602.5	30.3
SO239_135_ROV09	GSR	SM: Heip	3900-3550	1000m	6905.4	5.3
S0239_141_ROV10	GSR	NF	4455-4480	520m	1683.4	27.6
S0239_189_ROV13	APEI 3	NF	4890-4930	1790m	3580.0	3.8
S0239_200_ROV14	APEI 3	NF	4650-4670	1490m	2980.0	6.2
SO239_212_ROV15	APEI 3	SM: Mann Borgese	1850-1650	900m	4805.3	7.6

585 Table 2. Overview of all densities (ind./100m^2) observed within each video transect. Higher taxa are
586 in bold. * indicates taxa left out of the statistical analyses due to lack of representativity. Indets were
587 organisms impossible to attribute to a lower taxonomic group. ROV02=Rüppel, ROV04=Senkcenberg,
588 ROV09=Heip, ROV15=Mann Borgese

589

590

591

592

593

594

595

596

597

598

599

600

601

602

603

604

	SEAMOUNTS				NODULE FIELDS				
	ROV2 Ind./100m^2	ROV4 Ind./100m^2	ROV9 Ind./100m^2	ROV15 Ind./100m^2	ROV3 Ind./100m^2	ROV8 Ind./100m^2	ROV10 Ind./100m^2	ROV13 Ind./100m^2	ROV14 Ind./100m^2
Annelida*									
Polychaeta indet. * (No Serpulidae)	0.02	0.02		0.02	0.09		0.12	0.03	0.03
Acrocirridae	0.02	0.03	0.52		0.17	0.06	0.18	0.89	0.97
Aphroditidae	0.03	0.01							
Echiura msp 1					0.17	0.50	0.36		0.10
Polynoidea									
Polynoidae msp 2						0.06	0.18		
Polynoidae white msp						0.06		0.03	0.07
Bryozoa									
Bryozoa msp 2			0.02						
Bryozoa indet.		0.01			0.13	0.69	0.06	0.06	0.07
Cnidaria									
Anthozoa									
Ceriantharia									
Ceriantharia msp 1	0.04	0.01	0.05	0.04		0.06			
Ceriantharia msp 2				0.08		0.12	0.06		
Ceriantharia indet.			0.01						
Hexacorralia									
Actiniaria									
Actinoscyphiidae		0.02							
Actiniidae/*Bolocera* msp.	0.13	0.04							
Actiniaria msp 15	0.01								
Actiniaria msp 4		0.02		0.02					
Actiniaria msp 5	0.01	0.02		0.06					

Actiniaria msp 10					0.09				0.17
Actiniaria msp 2					0.32	0.50	0.06		0.13
Actiniaria msp C					0.11	0.19	0.12		
Actiniaria msp D					0.02				
Actiniaria msp 7					0.19	0.06	0.18	0.03	0.07
Actiniaria msp 8					0.04	1.62	0.95		0.10
Actiniaria msp 9							0.06		
Actiniaria msp A							0.06		0.03
Actiniaria msp B					0.08	0.06	0.12	0.03	
Actiniaria indet.	0.02	0.03			0.47	0.62	1.37	0.06	0.07
Antipatharia									
Antipathidae									
Antipathes msp 1				1.59					
Antipathes msp 2				0.02					
Stichopathes msp 1				1.75					
Antipathidae indet.				0.10					
Schizopathidae									
Abyssopathes cf. *lyra*					0.15	0.25	0.18		
Bathypathes cf. *alternata*						0.06	0.06		0.03
Bathypates cf. *alternata* msp 1			0.01						
Bathypathes cf. *alternata* msp 2		0.02							
Bathypathes sp.					0.06	0.06			
Bathypathes msp 1			0.01						
cf. *Parantipathes* msp 1			0.02						
Umbellapathes aff. *bipinnata*		0.04	0.01						
Umbellapathes aff. *helioanthes*		0.12							
Antipatharia indet.	0.01	0.02	0.01	0.12	0.08	0.12	0.06		
Corallimorpharia/Corallimorphidae									
Corallimorphus msp 1		0.01							
Corallimorphus msp 2		0.09	0.01		0.08	0.12	0.06		
Corallimorpharia msp 3		0.01							

Corallimorpharia msp 4			0.01						
Corallimorpharia msp A					0.02		0.06		
Corallimorpharia msp B					0.02				
Scleractinia									
Scleractinia msp 1	0.02			1.47					
Zoantharia									
Zoantharia msp 2				0.02					
Zoantharia indet.		0.09		0.04					
Octocorralia									
Alcyonacea									
Alcyoniidae									
Anthomastus msp 1	0.03								
Anthomastus msp 2	0.00	0.03		0.02					
Coralliidae									
Corallium sp. nov.				0.02					
Chrysogorgiidae									
Chrysogorgia cf. *pinnata*			0.01						
Isididae									
Bathygorgia aff. *abyssicola* 1						0.06	0.06		
Bathygorgia aff. *profunda* 1		0.03	0.01						
Bathygorgia aff. *profunda* 2			0.01						
Keratoisis aff. *flexibilis* msp 2			0.01						
Isididae msp 1		0.01							
Isididae indet.	0.02		0.11	0.02	0.04	2.50	0.71		
Taiaroidea									
Taiaroidae msp 1							0.06		
Primnoidae									
Abyssoprimnoa cf. *gemina*						0.31	0.18		
Callozostron cf. *bayeri*	0.01	0.11			0.02				
Calyptrophora cf. *persephone*					0.02				
Narella msp 1		0.02		0.02					

Primnoidea indet.	0.08		0.02		0.81	1.50	0.48		
Alcyonacea msp 1					0.04			0.06	0.07
Alcyonacea indet.		0.03	0.21	0.50	2.67	2.93	1.25		0.03
Pennatulacea									
Umbellulidae									
Umbellula msp 1_White									0.07
Umbellula msp 1_orange		0.06		0.02					
Umbellula msp 2		0.02							
Umbellulidae indet.		0.03							
Protoptilidae				0.02					
Protoptilum msp 1		0.01		0.04					
Pennatulacea msp 2		0.01							
Pennatulacea msp 5		0.05							
Pennatulacea msp 6		0.02							
Pennatulacea msp 7		0.08							
Pennatulacea msp 8		0.02							
Pennatulacea indet	0.02	0.42		0.02		0.06			
Octocorallia msp 1				0.04					
Octocorallia msp 2									
Anthozoa indet.	0.02	0.02	0.07	0.12	0.04	0.06	0.06		
Hydrozoa									
Branchiocerianthus msp		0.02							
Hydrozoa indet.		0.02	0.01	0.04		0.06			
Crustacea*									
Decapoda									
Caridea	0.46	0.52	0.47	0.04	0.06		0.36	0.06	0.10
Decapoda msp 3		0.02							
Decapoda msp 4	0.01								
Decapoda/Aristeidae	0.01	0.02		0.10	0.02	0.25	0.18	0.06	0.03
Decapoda msp 1								0.03	

Galatheidae									
Galatheidae small red msp	0.37	0.11	0.02	0.08	0.02				
Galatheidae small white msp	0.01	0.02							
Munidopsis spp.	0.11	0.07	0.07			0.19			0.10
Galatheidae indet.	0.02	0.03	0.02	0.02					
Parapaguridae									
Parapaguridae msp 1/*Probeebei* sp.	0.07	0.05							
Peracarida									
Amphipoda			0.01		0.02	0.12		0.03	0.13
Podoceridae msp 1								0.03	
Amphipoda msp 1		0.02	0.02						
Isopoda									
Munnopsidae msp 1					0.17	0.19	0.06	0.08	0.27
Decapoda indet.		0.02	0.10						
Crustacea indet.	0.01	0.06	0.07						0.07
Echinodermata									
Asteroidea									
Brisingida									
Brisingida msp 1 (6 arms - orange)		0.03	0.07		0.08				
Brisingida msp 1 (8 arms - orange)	0.02	0.08	0.04						0.03
Brisingida msp 3 (6 arms - white)		0.08	0.13	0.04	0.06	0.19	0.06		0.07
Brisingida msp 4 (9-10 arms)	0.02	0.08							
Brisingida indet.	0.04	0.02		0.04					
Paxillosida									
Solaster msp		0.01							
Paxillosida cf AST_009/AST_007		0.10	0.06						
Paxillosida msp 1	0.01			0.02					
Paxillosida msp 2a		0.01							
Paxillosida msp 2b			0.01						
Paxillosida msp 3		0.02	0.02						

Paxillosida msp 4		0.02							
Paxillosida msp 1								0.03	
Paxillosida indet.		0.13							
Velatida									
Pterasteridae									
Hymenaster msp 2	0.01								
Pteraster msp	0.03								
Velatida cf. AST_014	0.02	0.04							
Velatida msp 2							0.06		
Velatida msp 3									0.03
Asteroidea indet.	0.06	0.09	0.16	0.02	0.06				
Crinoidea									
Comatulida									
Bourgueticrinina msp 1					0.09				0.07
Comatulida msp 1	0.26	0.31					0.06		
Comatulida msp 2									0.07
Hyocrinida									
Hyocrinidae small msp					0.11	0.12			
Hyocrinidae msp 1		0.04	0.01						
Crinoidea red msp	0.03	0.33		0.08					
Crinoidea golden msp	0.02	0.08							
Crinoidea msp 1									0.03
Crinoidea indet.	0.01	0.09	0.01	0.02		0.06			
Echinoidea									
Aspidodiadematidae									
Aspidodiadematidae msp 1					1.19	1.19	0.71		
Aspidodiadematidae msp 2		0.04				0.06			
Aspidodiadematidae soft msp				0.02					
Aspidodiadematidae spiny msp	0.02			0.14					
Urechinidae									
Urechinidae msp 1_Nodules									0.03

Urechinidae msp 3	0.03	0.01	0.13						
Urechinidae msp 2_Nodules									0.03
Urechinidae msp 3_Nodules					0.02				
Urechinidae msp 4_Nodules								0.03	0.07
Urechinidae msp 1	0.03	0.15	0.04						
Urechinidae msp 2	0.03	0.01							
Urechinidae msp 4	0.06	0.28	0.06						
Urechinidae msp 5	0.01								
Urechinidae msp 6	0.01								
Urechinidae msp 7	0.01								
Urechinidae indet.	0.02	0.02	0.01						
Echinoidea indet.	0.01								
Holothuroidea									
Elasipodida									
Elpidiidae									
Elpidiidae double-velum msp							0.06		
Elpidiidae msp 1								0.03	0.03
Amperima msp	0.02								
Amperima msp 1					0.02				
Peniagone "palmata" msp						0.06	0.12		
Peniagone "tulip" msp							0.06		
Peniagone cf. *leander*						0.06	0.06		
Peniagone msp	0.02	0.02							
Peniagone purple msp									0.03
Peniagone white/transparent msp					0.02			0.03	0.03
Peniagone indet.					0.04				
Laetmogonidae									
Laetmogonidae msp 1	0.04	0.09							
Laetmogonidae msp 2	0.03								
Laetmogonidae msp 3							0.06		0.03
Pelagothuriidae									

Enypniastes sp.									0.03
Psychropotidae									
Benthodytes cf. *incertae* purple msp		0.03	0.01						
Benthodytes cf. *incertae* red msp		0.09							
Benthodytes msp		0.04							
Benthodytes msp 1									0.03
Benthodytes pink msp				0.02					
Benthodytes purple msp			0.01						
Benthodytes red msp		0.01	0.01						
Psychropotes cf. *semperiana*								0.03	
Psychropotes longicauda							0.12		
Psychropotes msp 3					0.02		0.06		
Psychropotes verrucosa					0.08	0.06			
Psychropotidae msp 1_Nodules					0.02	0.06	0.06		
Psychropotidae msp 1		0.07	0.01						
Psychropotidae msp 2_Nodules						0.19			
Psychropotidae msp 2		0.01							
Psychropotidae msp 3					0.04	0.06			
Psychropotidae msp 4						0.06			
Psychropotidae red msp	0.02								
Psychropotidae indet.	0.16	0.09		0.02					
Holothuriida									
Mesothuriidae									
Mesothuria msp	0.01	0.02							
Synallactida									
Deimatidae									
Deima msp.		0.01							
Deimatidae - irregular papillae length msp		0.05	0.01						
Oneirophanta msp	0.01		0.02						
Deimatidae indet.		0.01	0.01						
Synallactidae									

Benthothuria msp				0.08					
Paelopatides "orange" msp	0.01	0.01							
Synallactes msp 1 (Synallactidae purple msp)	0.01								
Synallactes msp 2		0.01							
Synallactes msp 2 pink					0.04	0.25	0.06		
Synallactes msp 2 pink (smooth)	0.03	0.02				0.31			
Synallactes sandy-coloured msp	0.02								
Synallactes white msp	0.02				0.70	0.19	0.30		0.03
Synallactidae indet.	0.04								
Persiculida									
Molpadiodemidae									
Molpadiodemas msp		0.02							
Pseudostichopodidae									
Pseudostichopus msp						0.06			
Molpadiodemas/Mesothuria					0.06	0.12	0.06		0.07
Holothuroidea indet.	0.17	0.15	0.04	0.04	0.06	0.06	0.12		
Ophiuroidea									
Ophiuroidea msp 1					0.02	0.06	0.06		
Ophiuroidea msp 3						0.12			
Ophiuroidea msp 5	0.02	0.39	0.49					0.03	0.10
Ophiuroidea msp 6		0.03	0.01		0.32	1.31	0.65	0.17	0.44
Ophiuroidea msp 4	0.04	0.21			0.11				
Ophiuroidea msp7		0.01							
Ophiuroidea indet.		0.02	0.04	0.08	5.67	6.68	7.31		0.13
Enteropneusta									
Enteropneusta msp 1 cf. *Yoda*		0.10							
Enteropneusta msp 2 cf. *Saxipendum* msp.	0.07								
Mollusca									
Gastropoda									

Limpet			0.01						
Gastropoda msp 1			0.02						
Polyplacophora	0.04			0.04					0.07
Gastropoda indet.						0.06			
Cephalopoda									
Octopoda msp 1	0.01								
Pisces*	0.33	0.28	0.07	0.06	0.47	0.19	0.48	0.17	0.17
Porifera									
Demospongiae									
Cladorhizidae									
Cladorhizidae msp 1			0.02						0.07
Cladorhizidae msp 1(soft)									0.03
Cladorhizidae msp 2								0.03	0.03
Cladorhizidae msp 3									0.03
Cladorhizidae msp 4					0.02			0.06	0.13
Cladorhizidae msp 5						0.06			
Cladorhizidae msp 6						0.06			
Cladorhizidae indet								0.03	0.07
Hexactellinida									
Euplectellidae									
Bathydorus spinosus	0.01								
Bolosoma sp.				0.02					
Corbitella discasterosa	0.01							0.06	
Docosaccus maculatus						0.06		0.03	
Docosaccus nidulus						0.06			
*Holascus*spp					0.19	0.12	0.06	0.03	0.03
Hyalostylus schulzei								0.03	
Hyalostylus sp.		0.02	0.15	0.02				0.03	0.03
Sacocalyx pedunculatus				0.06					

Sacocalyx sp.	0.04	0.02	0.02						
Euretidae									
Bathyxiphus subtilis								0.03	
Chonelasma bispinula							0.06		
Chonelasma choanoides	0.01								
Chonelasma sp.			0.01						
Hyalonematidae									
Hyalonema spp.		0.02	0.10	0.02	0.11	0.31	0.24	0.08	0.23
Rosselidae									
Caulophacus sp.		0.06	0.07	0.02	0.17	0.06	0.06		
Crateromorpha sp.		0.02		0.02					
Rossellidae gen. sp.	0.04	0.01	0.02						
Pheronematidae									
Poliopogon sp.				0.02					
Hexactellinida/foliose sponge msp	0.01	0.02	0.01	0.06					
Hexactellinida - Stalked					0.26	0.50	0.53		
Hexactinellida black msp		0.01							
Hexactellinida indet.	0.20	0.20	0.52	0.12	0.98	1.06	1.60	0.45	0.37
Pycnogonida	0.02		0.01						0.03
Tunicata									
Octacnemidae									
Megalodicopia msp. 1	0.02	0.01	0.01						
Megalodicopia msp. 2									0.03
Dicopia msp.	0.04								
Pyuridae									
Culeolus msp.									0.03
Tunicata indet.	0.02	0.01	0.01	0.02					
Paleodictyon nodosum								0.03	

605

Figures

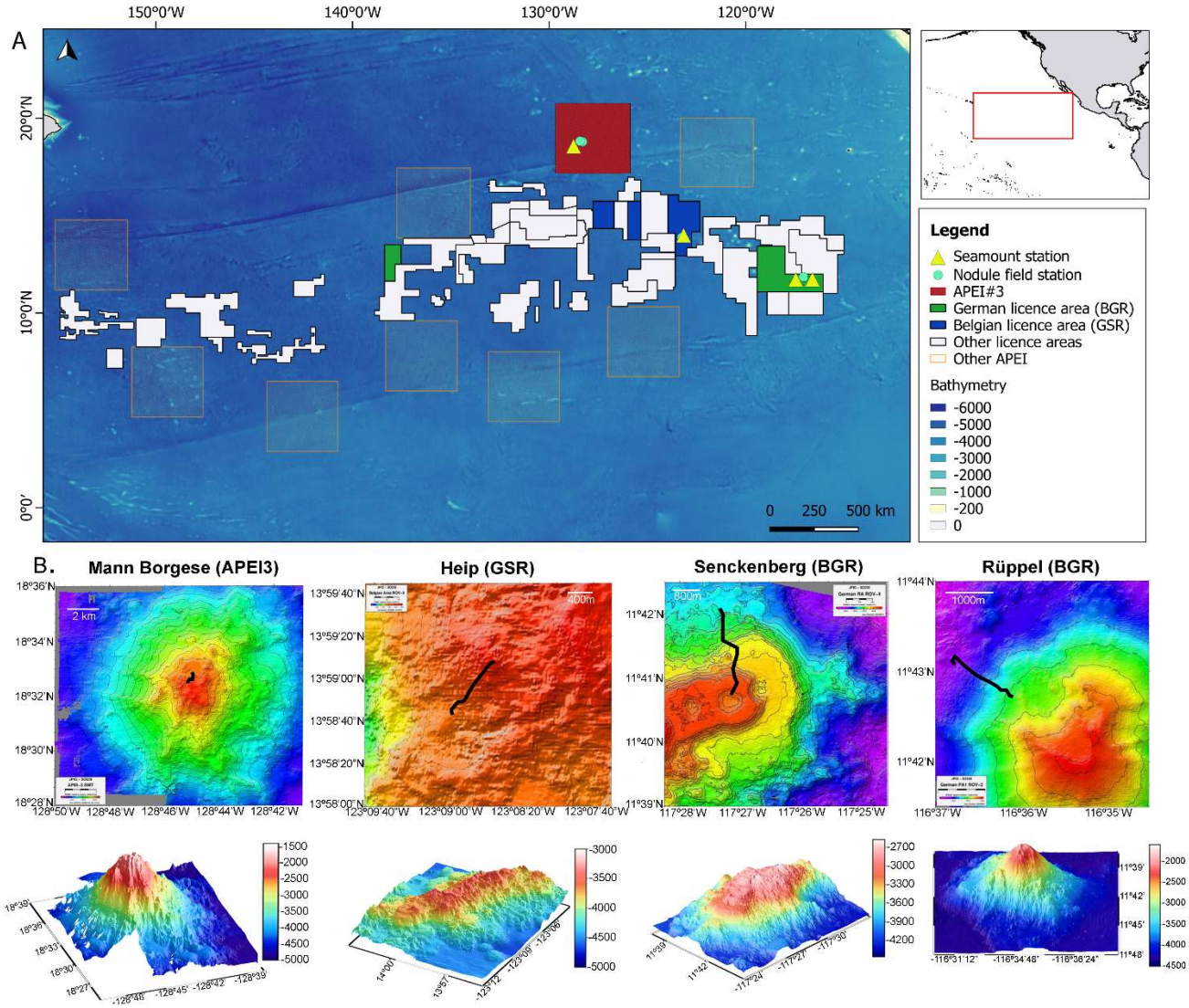

Fig. 1. (A). Location of the Clarion-Clipperton Fracture zone in the equatorial eastern Pacific Ocean featuring the contract areas from the International Seabed Authority (ISA) and the positions of the sampled areas (seamounts and nodule fields). Information on transect length and depth gradients can be found in Table 1. (B). Location of the seamount transects carried out towards the summit on the north –north-western flank and seamount profiles. Rüppel (BGR, ROV02) and Mann Borgese (APEI3, ROV15) are single seamounts, while Senckenberg (BGR, ROV04) and Heip (GSR, ROV09) are sea-mountain ranges.

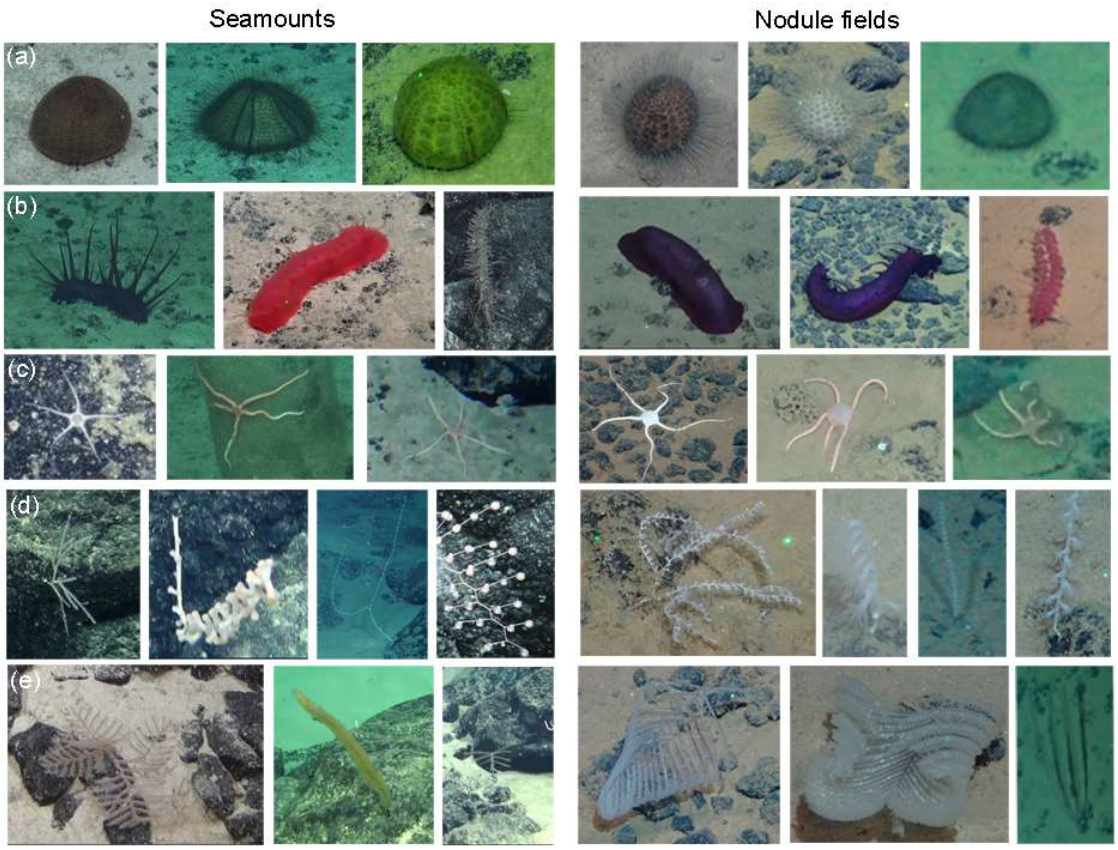

Fig. 2. Some examples of different morphospecies at seamounts and nodule fields in the CCZ. Selected taxa were (a) Echinoidea (from left to right, Urechinidae msp 4 (URC_019), Urechinidae msp 2 (URC_013), Urechinidae msp 3 (URC_009), Urechinidae msp. A (URC_020), Urechinidae msp. B (URC_021), Urechinidae msp. C (URC_005), (b) Holothuroidea (from left to right, Psychropotidae msp 1 (HOL_088), *Benthodytes* red msp. (HOL_101), Deimatidae - irregular papillae msp. (HOL_070), *Psychropotes verrucosa* (HOL_045), Laetmogonidae (HOL_030), *Synallactes* msp 2 pink (HOL_008)(c) Ophiuroidea (from left to right, Ophiuroidea msp. 5 (OPH_003), Ophiuroidea msp. 4 (OPH_005), Ophiuroidea msp. 6 (OPH_006), Ophiuroidea msp. 6 (OPH_006), Ophiuroidea (OPH_012), Ophiuroidea msp. 4 (OPH_005)), (d) Alcyonacea (from left to right, *Callozostron* cf. *bayeri (*ALC_009), *Bathygorgia* aff. *profunda* 2 (ALC_005), *Keratoisis* aff. *flexibilis* msp 2 (ALC_029), *Chrysogorgia* cf. *pinnata*, *Abyssoprimnoa* cf. *gemina* (ALC_008), *Bathygorgia* aff. *profunda* 1, *Calyptrophora* cf. *persephone* (ALC_007), *Bathygorgia* aff. *abyssicola* 1 (ALC_003), (e) Antipatharia (*Umbellapathes* aff. *helioanthes* (ANT_018), cf. *Parantipathes* morphotype 1 (ANT_017), *Bathypates* cf. *alternata* msp 1 (ANT_010), *Bathypathes* cf. *alternata* (ANT_006), *Abyssopathes* cf. lyra (ANT_022), *Bathypathes* sp. (ANT_003)). Codes refer to an ongoing collaboration in creating one species catalogue for the CCZ and align all morphospecies of different research groups. Copyright: SO239, ROV Kiel 6000, GEOMAR Helmholtz Centre for Ocean Research Kiel

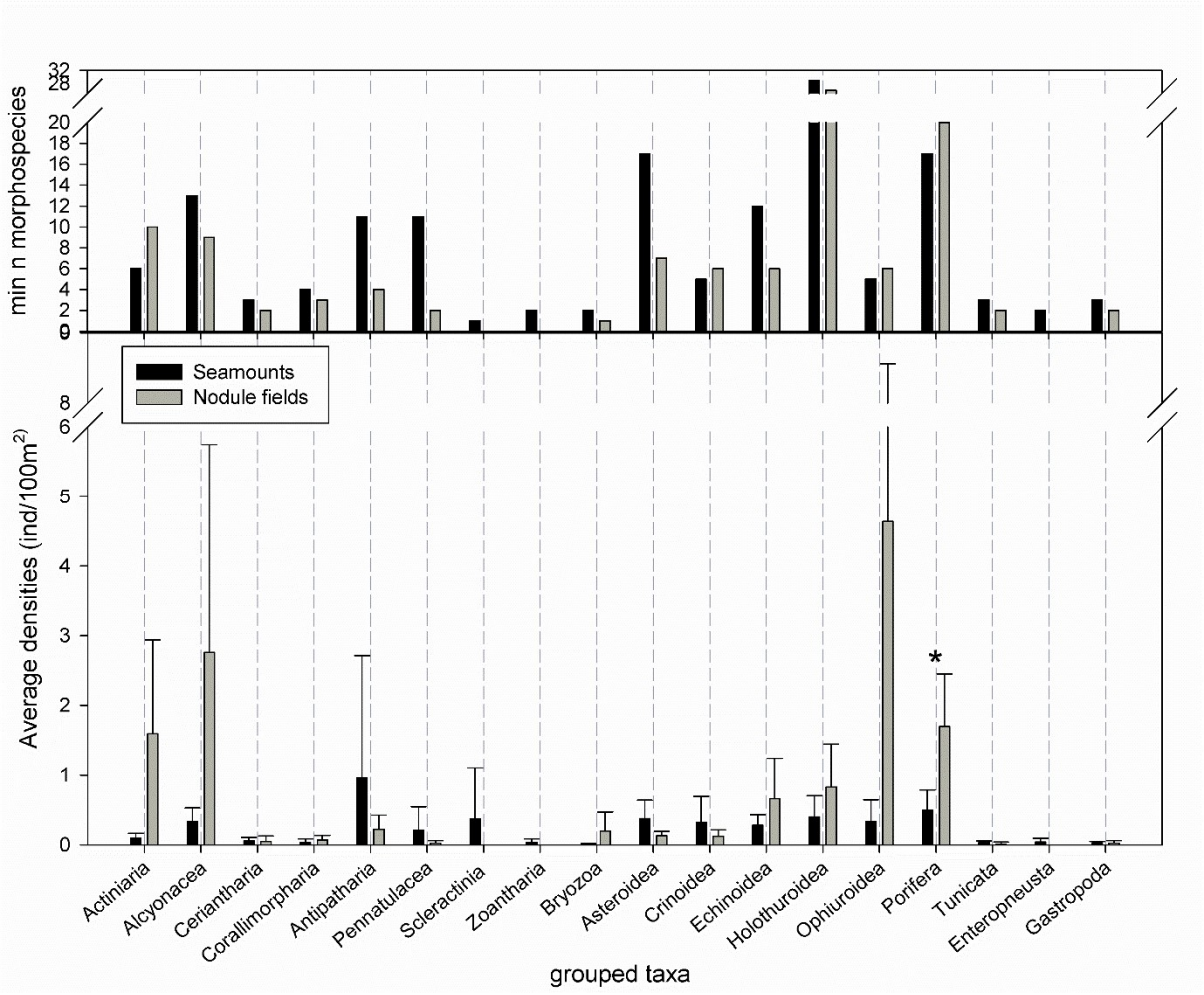

637

638 Fig. 3. Average densities at higher taxa level per ecosystem and standard deviation in the lower
639 panel and minimum number of morphospecies per taxon and ecosystem in the upper panel. *=
640 Significant difference in density ($t=-3.7$, $p<0.05$).

641

642

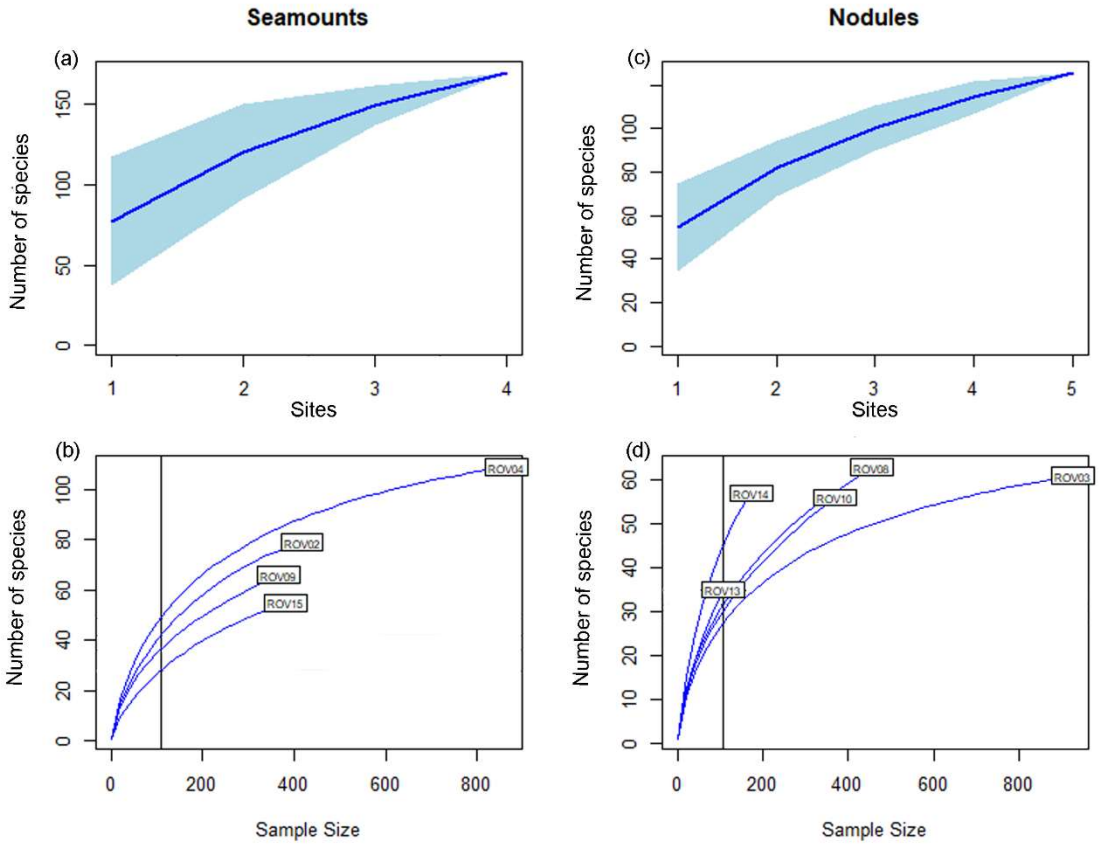

643
644 Fig. 4. Species accumulation (upper panel, a and c) and rarefaction curves (lower panel, b and d) for
645 the seamount (n=4) and nodule field (n=5) transects. Seamount dives: ROV02= Rüppel (BGR),
646 ROV04=Senckenberg (BGR), ROV09=Heip (GSR), ROV15=Mann Borgese (APEI3) in the lower left
647 panel (b). Nodule field dives: ROV03 was carried out in the BGR area, ROV08 and 10 in the GSR area
648 and ROV13 and 14 in the APEI3, presented in the lower right panel (d). Sample size is the number of
649 individuals. Vertical line in the lower panel shows sample size=100.

650

651

652

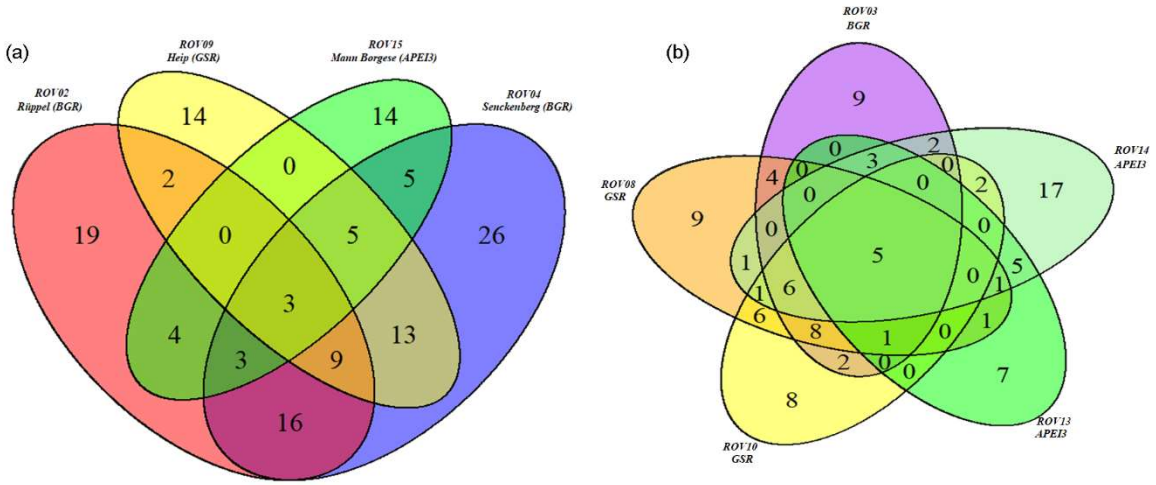

Fig. 5. A Venn diagram showing the unique and shared morphospecies among seamount video transects. Values are indicative rather than absolute due to different transect lengths and differences in richness. Left panel (a) features seamount transects and the right panel features the 5 nodule field transects. Colour codes were adapted among panels, with APEI3 nodule transects in green, related to Mann Borgese seamount transect. BGR (ROV03) transect was purple in correspondence to BGR seamount transects (red=Rüppel and blue=Senckenberg). GSR transects (ROV08 and 09) were shades of yellow.

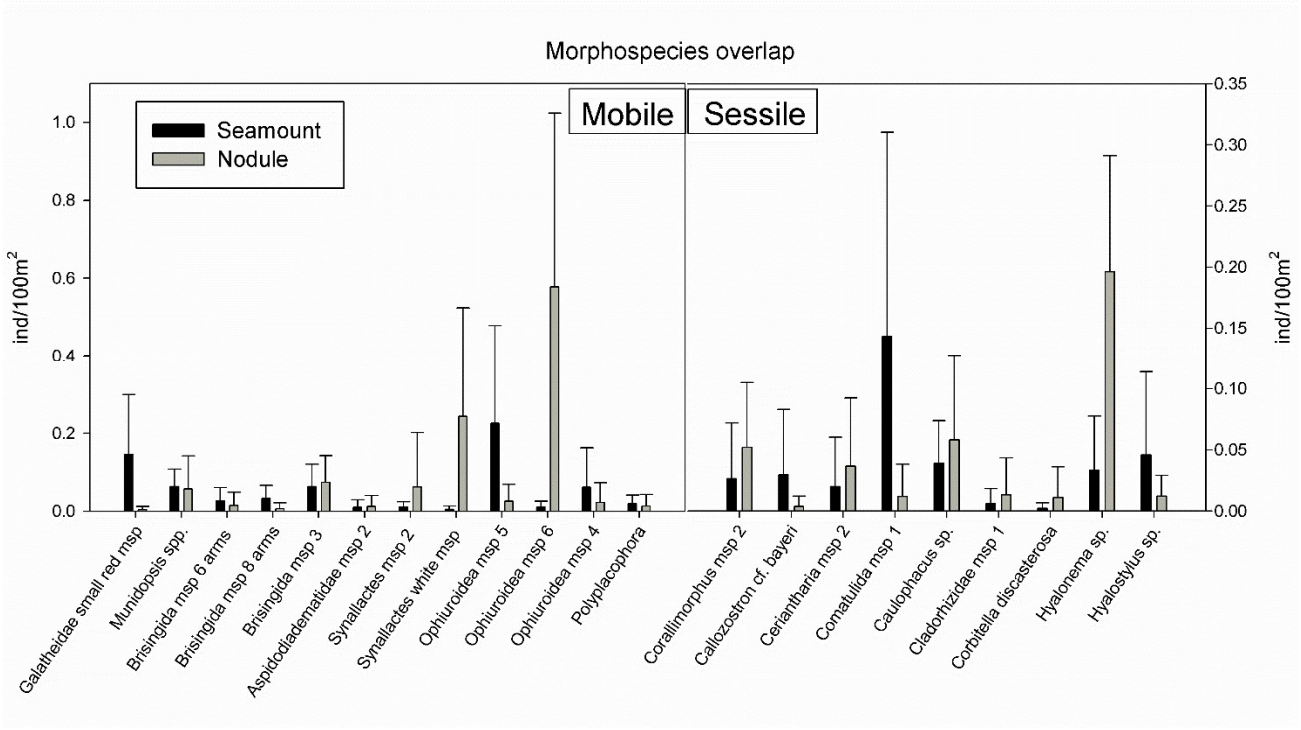

666

667 Fig. 6. Morphospecies present in both seamounts and nodule field transects and their average
668 density (ind./100m^2) and standard deviation per ecosystem.

669

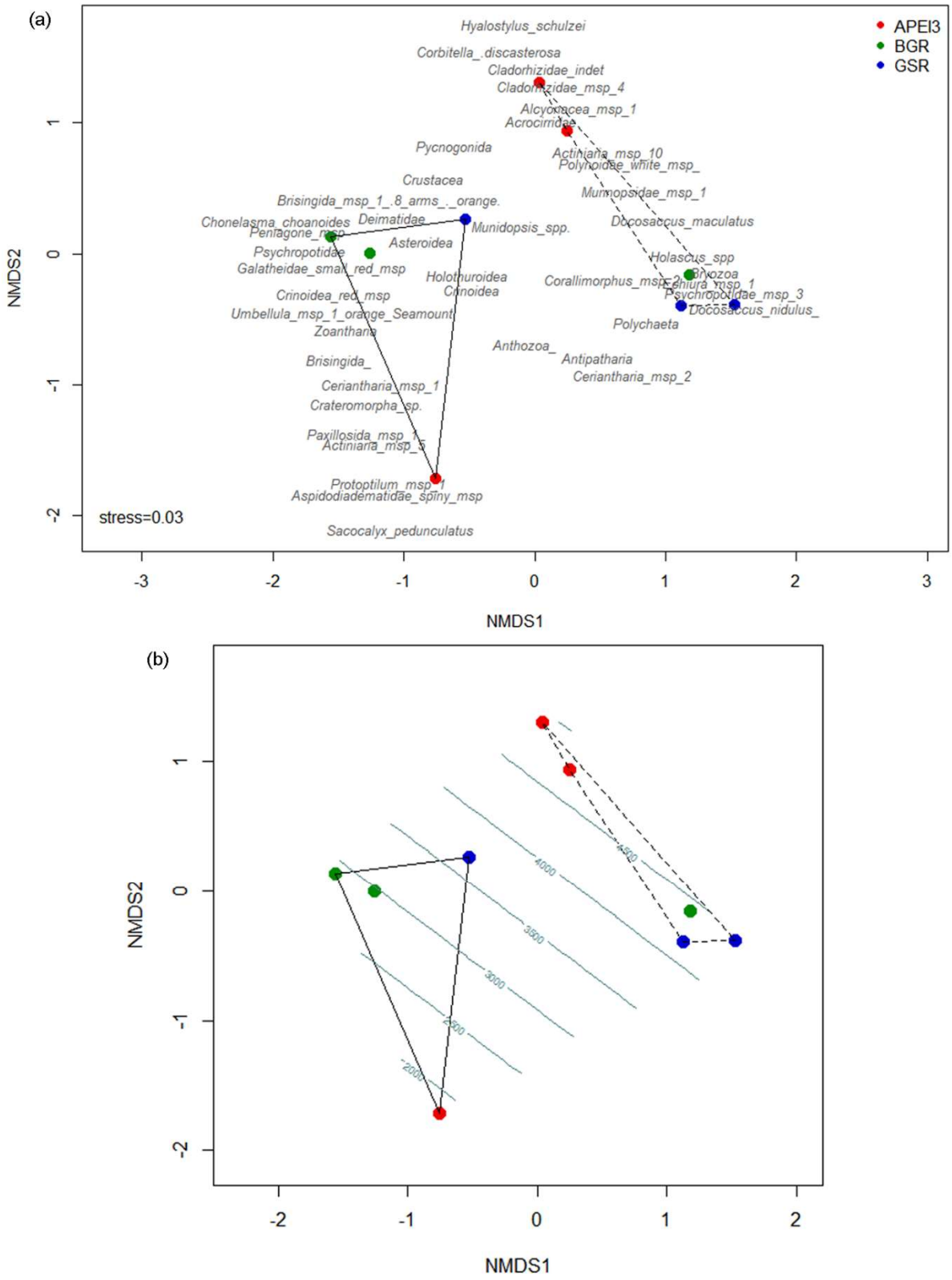

670

671 Fig. 7. nMDS-plot with faunal densities and Bray-Curtis distances. Upper panel (a) presents the
672 grouping of the video transects based on their faunal composition and lower panel (b) features the

673 same plot but with depth as a vector fitting. Dotted lines group the nodule transects while the full
674 line groups the seamount transects.

675

676

677

Appendix

.

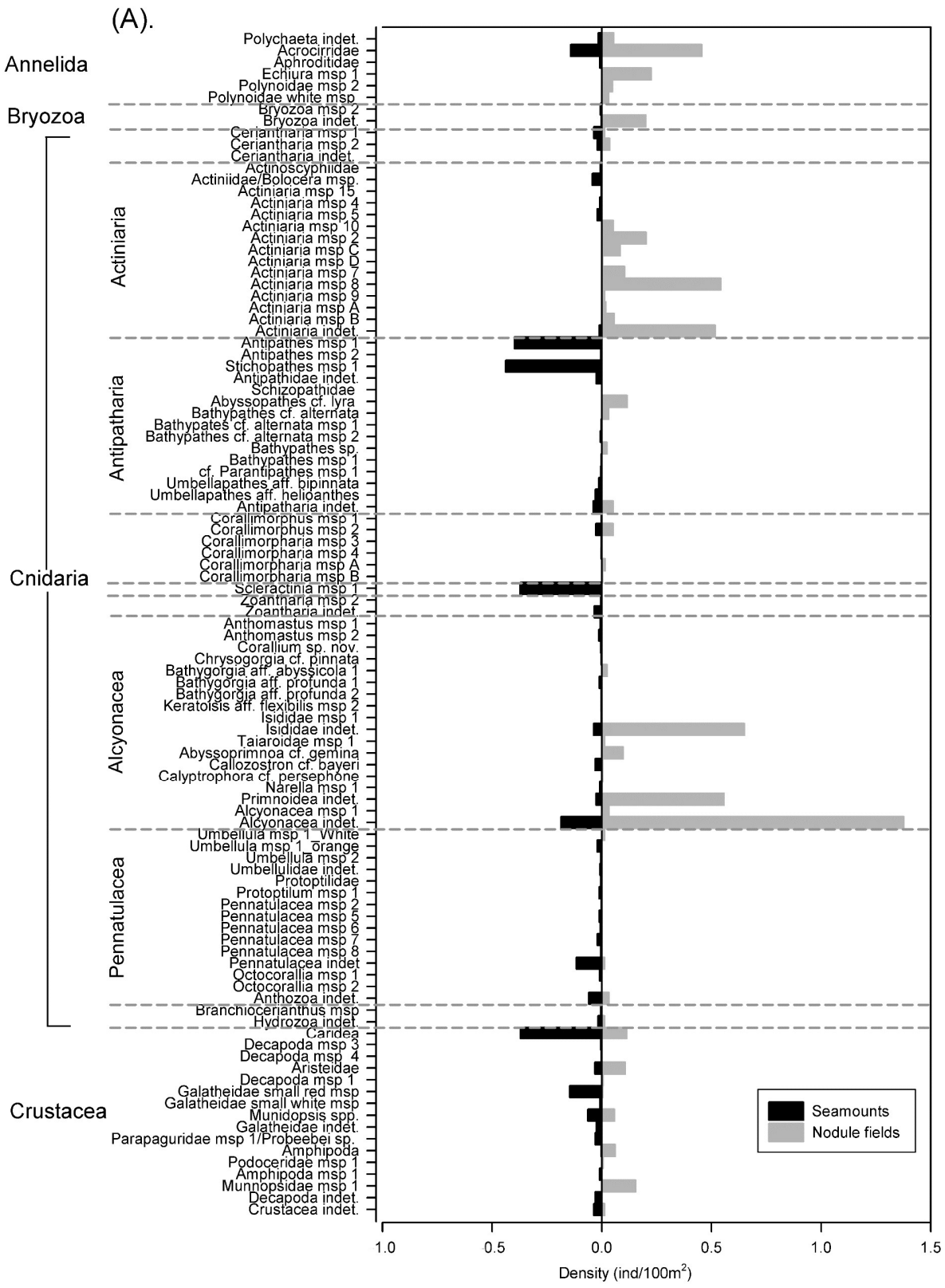
(A).
Annelida
Bryozoa
Cnidaria
Crustacea
Actiniaria
Antipatharia
Alcyonacea
Pennatulacea
Polychaeta indet.
Acrocirridae
Aphroditidae
Echiura msp 1
Polynoidae msp 2
Polynoidae white msp
Bryozoa msp 2
Bryozoa indet.
Ceriantharia msp 1
Ceriantharia msp 2
Ceriantharia indet.
Actinoscyphiidae
Actiniidae/Bolocera msp.
Actiniaria msp 15
Actiniaria msp 4
Actiniaria msp 5
Actiniaria msp 10
Actiniaria msp 2
Actiniaria msp C
Actiniaria msp D
Actiniaria msp 7
Actiniaria msp 8
Actiniaria msp 9
Actiniaria msp A
Actiniaria msp B
Actiniaria indet.
Antipathes msp 1
Antipathes msp 2
Stichopathes msp 1
Antipathidae indet.
Schizopathidae
Abyssopathes cf. lyra
Bathypathes cf. alternata
Bathypates cf. alternata msp 1
Bathypathes cf. alternata msp 2
Bathypathes sp.
Bathypathes msp 1
cf. Parantipathes msp 1
Umbellapathes aff. bipinnata
Umbellapathes aff. helioanthes
Antipatharia indet.
Corallimorphus msp 1
Corallimorphus msp 2
Corallimorpharia msp 3
Corallimorpharia msp 4
Corallimorpharia msp A
Corallimorpharia msp B
Scleractinia msp 1
Zoantharia msp 2
Zoantharia indet.
Anthomastus msp 1
Anthomastus msp 2
Corallium sp. nov.
Chrysogorgia cf. pinnata
Bathygorgia aff. abyssicola 1
Bathygorgia aff. profunda 1
Bathygorgia aff. profunda 2
Keratoisis aff. flexibilis msp 2
Isididae msp 1
Isididae indet.
Taiaroidae msp 1
Abyssoprimnoa cf. gemina
Callozostron cf. bayeri
Calyptrophora cf. persephone
Narella msp 1
Primnoidea indet.
Alcyonacea msp 1
Alcyonacea indet.
Umbellula msp 1_White
Umbellula msp 1_orange
Umbellula msp 2
Umbellulidae indet.
Protoptilidae
Protoptilum msp 1
Pennatulacea msp 2
Pennatulacea msp 5
Pennatulacea msp 6
Pennatulacea msp 7
Pennatulacea msp 8
Pennatulacea indet
Octocorallia msp 1
Octocorallia msp 2
Anthozoa indet.
Branchiocerianthus msp
Hydrozoa indet.
Caridea
Decapoda msp 3
Decapoda msp 4
Aristeidae
Decapoda msp 1
Galatheidae small red msp
Galatheidae small white msp
Munidopsis spp.
Galatheidae indet.
Parapaguridae msp 1/Probeebei sp.
Amphipoda
Podoceridae msp 1
Amphipoda msp 1
Munnopsidae msp 1
Decapoda indet.
Crustacea indet.
Seamounts
Nodule fields
1.0
0.5
0.0
0.5
1.0
1.5
Density (ind/100m^2)

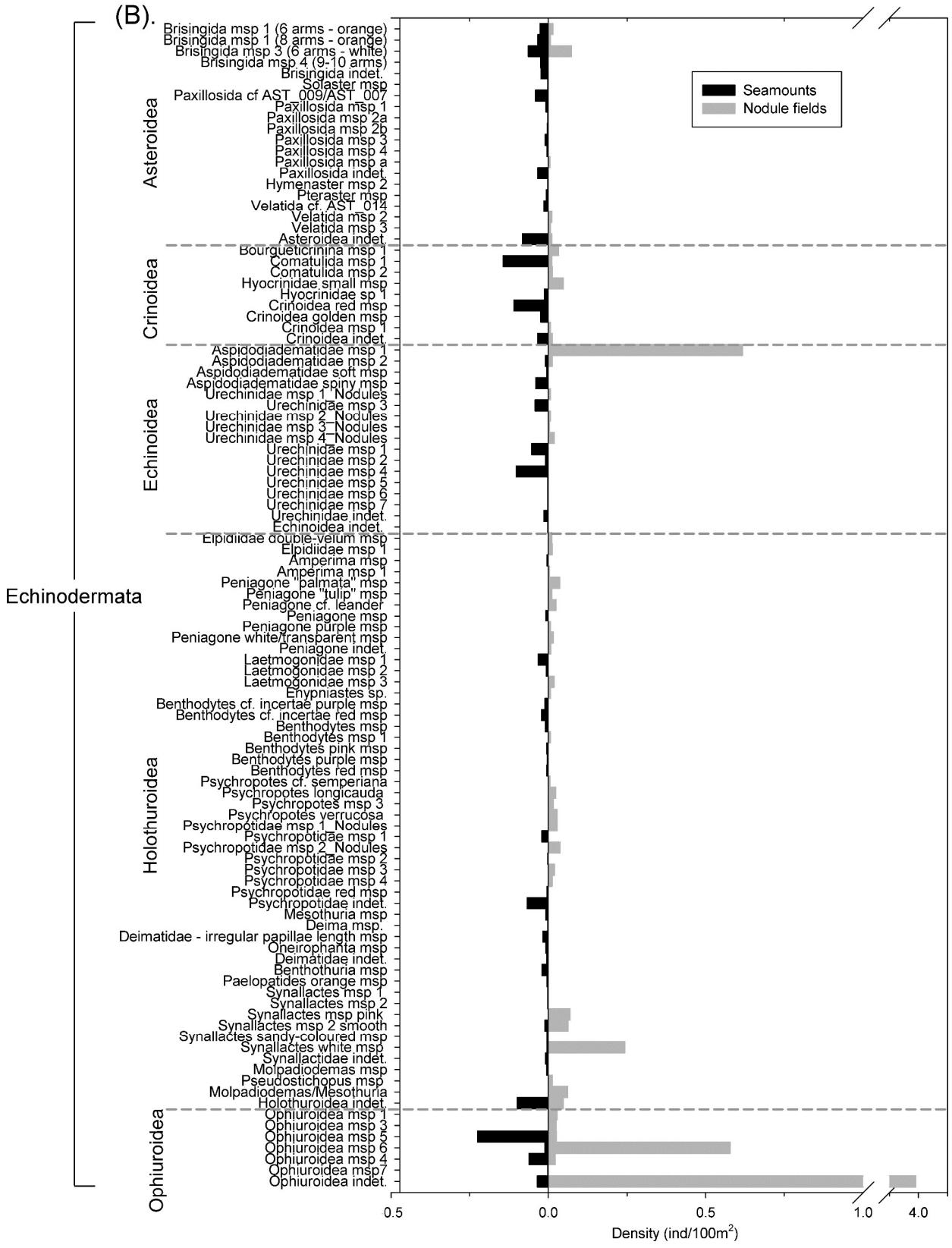
(B).
Echinodermata
Asteroidea
Crinoidea
Echinoidea
Holothuroidea
Ophiuroidea
Brisingida msp 1 (6 arms - orange)
Brisingida msp 1 (8 arms - orange)
Brisingida msp 3 (6 arms - white)
Brisingida msp 4 (9-10 arms)
Brisingida indet.
Solaster msp
Paxillosida cf AST_009/AST_007
Paxillosida msp 1
Paxillosida msp 2a
Paxillosida msp 2b
Paxillosida msp 3
Paxillosida msp 4
Paxillosida msp a
Paxillosida indet.
Hymenaster msp 2
Pteraster msp
Velatida cf. AST_014
Velatida msp 2
Velatida msp 3
Asteroidea indet.
Bourgueticrinina msp 1
Comatulida msp 1
Comatulida msp 2
Hyocrinidae small msp
Hyocrinidae sp 1
Crinoidea red msp
Crinoidea golden msp
Crinoidea msp 1
Crinoidea indet.
Aspidodiadematidae msp 1
Aspidodiadematidae msp 2
Aspidodiadematidae soft msp
Aspidodiadematidae spiny msp
Urechinidae msp 1_Nodules
Urechinidae msp 3
Urechinidae msp 2_Nodules
Urechinidae msp 3_Nodules
Urechinidae msp 4_Nodules
Urechinidae msp 1
Urechinidae msp 2
Urechinidae msp 4
Urechinidae msp 5
Urechinidae msp 6
Urechinidae msp 7
Urechinidae indet.
Echinoidea indet.
Elpidiidae double-velum msp
Elpidiidae msp 1
Amperima msp
Amperima msp 1
Peniagone "palmata" msp
Peniagone "tulip" msp
Peniagone cf. leander
Peniagone msp
Peniagone purple msp
Peniagone white/transparent msp
Peniagone indet.
Laetmogonidae msp 1
Laetmogonidae msp 2
Laetmogonidae msp 3
Enypniastes sp.
Benthodytes cf. incertae purple msp
Benthodytes cf. incertae red msp
Benthodytes msp
Benthodytes msp 1
Benthodytes pink msp
Benthodytes purple msp
Benthodytes red msp
Psychropotes cf. semperiana
Psychropotes longicauda
Psychropotes msp 3
Psychropotes verrucosa
Psychropotidae msp 1_Nodules
Psychropotidae msp 1
Psychropotidae msp 2_Nodules
Psychropotidae msp 2
Psychropotidae msp 3
Psychropotidae msp 4
Psychropotidae red msp
Psychropotidae indet.
Mesothuria msp
Deima msp.
Deimatidae - irregular papillae length msp
Oneirophanta msp
Deimatidae indet.
Benthothuria msp
Paelopatides orange msp
Synallactes msp 1
Synallactes msp 2
Synallactes msp pink
Synallactes msp 2 smooth
Synallactes sandy-coloured msp
Synallactes white msp
Synallactidae indet.
Molpadiodemas msp
Pseudostichopus msp
Molpadiodemas/Mesothuria
Holothuroidea indet.
Ophiuroidea msp 1
Ophiuroidea msp 3
Ophiuroidea msp 5
Ophiuroidea msp 6
Ophiuroidea msp 4
Ophiuroidea msp7
Ophiuroidea indet.
Seamounts
Nodule fields
0.5
0.0
0.5
1.0
4.0
Density (ind/100m^2)

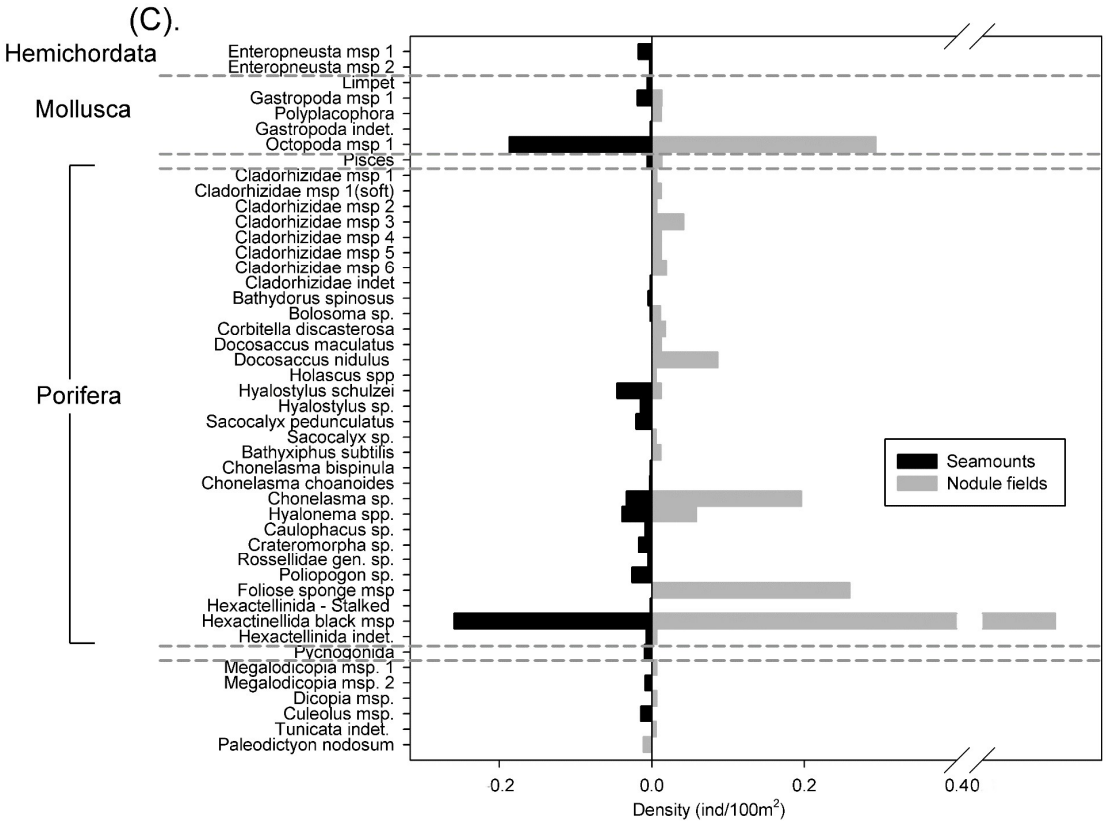

Fig. A1. Back-to-back histogram comparing average densities of morphospecies and taxa (ind/100m) for seamount (n=4) and nodule field (n=5) video transects. (A) Annelida, Bryozoa, Cnidaria and Crustacea, (B) Echinodermata and (C) Mollusca, Porifera, Hemichordata and Chordata (Tunicata).